THE SODDEN SWAMPS THAT SURROUND THEM: THREE ESSAYS CONCERNING THE LINKS BETWEEN RIVER CHANNELS AND THEIR OVERBANK ENVIRONMENTS

AN ABSTRACT

SUBMITTED ON THE FOURTH DAY OF AUGUST 2017

TO THE DEPARTMENT OF EARTH AND ENVIRONMENTAL SCIENCES

IN PARTIAL FULFILLMENT OF THE REQUIREMENTS

OF THE SCHOOL OF SCIENCE AND ENGINEERING

OF TULANE UNIVERSITY

FOR THE DEGREE

OF

DOCTOR OF PHILOSOPHY

BY

_____

CHRISTOPHER READ ESPOSITO

APPROVED: _____

Kyle M. Straub, Ph.D., Director

_____

Mead A. Allison, Ph.D.

_____

H.R. Albert Jagers, Ph.D.

_____

Torbjörn E. Törnqvist, Ph.D.

ABSTRACT

Though rivers are inextricably linked in our minds with an intermittently flooded overbank environment, surprisingly little is known about the sedimentary processes that operate there, or how they interact with those of the river. The knowledge gap is acute in deltas, where dense populations often necessitate tightly engineered control over flow patterns, leading to disconnected overbank environments that no longer receive input from the main channel. However, the need to understand sedimentary function in the overbank is also acute in deltas, as rising relative sea levels create an urgent need to manage water and sediment resources.

This dissertation is presented as three primary chapters, each of which examines a different aspect of the hydrodynamic and sedimentary connection between a river's channel and its overbank environment. In Chapter 2, my coauthors and I ask which factors enhance overbank sediment retention, and what retention rates might be considered typical in deltas. We compare the sediments stored in a crevasse splay to those transported by the river and conclude that retention rates approaching 100% might be achievable in settings that are not exposed to coastal processes. Chapter 4 is also concerned with spatial patterns of sedimentation on a delta. In it we use physical experiments to examine the influence that floods play in mobilizing sediments from the channel and storing them in the overbank environment. We find, counterintuitively, that an experiment whose input included floods has a lower proportion of floodplain to channel deposits preserved than an experiment with a constant input. Chapter 3 is focused on water and sediment dynamics in the channel in a region where significant flow is lost

to the overbank environment. Here we present measurements from channel networks in the Mississippi River's Birdsfoot Delta and show that flow loss along the channels is a critical control on channel function that causes channels of disparate sizes to behave similarly. We use our field results to inform a numerical model of channel bed evolution in a region with flow losses, and conclude that the modern flood control system in the Lower Mississippi River may have significantly changed the bed morphology.

THE SODDEN SWAMPS THAT SURROUND THEM: THREE ESSAYS CONCERNING THE LINKS BETWEEN RIVER CHANNELS AND THEIR OVERBANK ENVIRONMENTS

A DISSERTATION

SUBMITTED ON THE FOURTH DAY OF AUGUST 2017

TO THE DEPARTMENT OF EARTH AND ENVIRONMENTAL SCIENCES

IN PARTIAL FULFILLMENT OF THE REQUIREMENTS

OF THE SCHOOL OF SCIENCE AND ENGINEERING

OF TULANE UNIVERSITY

FOR THE DEGREE

OF

DOCTOR OF PHILOSOPHY

BY

_____

CHRISTOPHER READ ESPOSITO

APPROVED: _____

Kyle M. Straub, Ph.D., Director

_____

Mead A. Allison, Ph.D.

_____

H.R. Albert Jagers, Ph.D.

_____

Torbjörn E. Törnqvist, Ph.D.

Acknowledgements

To Margaret and Walker, my family.

To all who have so freely offered their time, their advice, their wit, their dexterity, and their strength. I offer my sincere thanks.

To my mentor and friend, Kyle Straub, who was kind enough once to tell me that I was "just the kind of student his lab could use" and that he hoped I would join. I hope that I have repaid his confidence.

Financial support for this work was generously given by Tulane's Department of Earth and Environmental Sciences via the Vokes Fellowship, and by the National Science Foundation through grants OCE-1049387 and EAR-1024443 to Straub, and EAR-1148005 to Shen and Törnqvist. Michael Blum and Shelley Meaux at the Center for Bioenvironmental Research were kind enough to allow me the liberal use of their boat and truck.

Table of Contents

List of Tables

List of Figures

1 Introduction

A thin blue line might reasonably be used to indicate a river on a map. The line would follow the course of the river's center, or perhaps of its banks, showing travelers exactly where further progress could only proceed by boat. But in most lowland settings a traveler taking the map's guidance literally would find the way to be difficult or impossible long before arriving at the riverbank. Indeed, for most net depositional environments the influence of the river extends far from the channel itself.

I use the phrase "overbank" or "overbank environment" in this dissertation to refer to the area adjacent to a river's channel that is intermittently impacted by floodwaters. The sedimentary processes in the overbank environment vary greatly, from violent levee breaches and crevasse splays, to quiet deposition in forested back swamps. But despite the variability in process, overbank environments in general are understood as sediment sinks that serve as important recorders of environmental signals from the river. Their proximity to the river's channel means that the characteristics of the overbank, including topography, vegetation, and the erodibility of sediment stored there, play an important role in determining fundamental qualities about the channel. These include whether or not the channel is able to erode its banks to move laterally, and whether the river forms a single channel or a braided stream. But while the channel exerts influence on the overbank environment, and vice versa, the dynamic interaction between the two has not often been studied. Each of the three papers that make up this dissertation

is intended to elucidate some aspect of the interaction between channels and their associated overbank environments.

Overbank environments are also important because they support dense human populations. Perhaps nowhere is the need to understand the sedimentary function of overbank environments more urgent than on river deltas, where broad expanses of flat, fertile land, fresh water, and easy access to navigation have historically supported large populations. However, the same features that make deltas uniquely attractive to human habitation make them uniquely vulnerable to the consequences of sea level rise. The risks are often exacerbated by overly strict river management techniques that have restricted the morphological evolution of river channels (e.g. Barry, 1998). To mitigate the risk of sea level rise, authorities in some deltas have concluded that loosening their control over the rivers and allowing them to interact more freely with their floodplain is a cost-effective way of protecting vulnerable locations. This strategy has been tried with some success in the tidal delta plain of the Ganges-Brahmaputra Delta (Auerbach et al., 2015) and in the Netherlands (Rijke et al., 2012), and is important to management plans in the Mississippi River Delta (Coastal Protection and Restoration Authority of Louisiana, 2017). Research conducted that enhances our understanding of how channels and overbank environments interact will pay dividends in the coming decades as coastal societies are forced to reshape land use patterns and redesign infrastructure to protect the lives, property, and culture of their citizens.

Chapter 2, "Efficient Retention of Mud Drives Land Building on The Mississippi Delta Plain", centers on the question of how effectively features on a delta plain retain the sediments that are delivered to them from the river. The answer to this

question has large implications for the sustainability of deltaic land as sea level rises. This work centers on a comparison of the sediments that are carried by a distributary of the Mississippi River with the sediments that are preserved in a large crevasse splay in the distributary's overbank environment, which my coauthors and I consider as an analog for the types of deposits that will be created by planned and managed river diversions. The comparison is informative because a deposit that is depleted in fine sediments compared to the river would indicate an environment that did not successfully trap incoming fine sediments. We find, however, that the composition of sediments preserved in the crevasse splay is similar to the composition of the sediments that were transported in suspension by the river that fed it, indicating very little loss of sediments through the downstream boundary of the crevasse splay. The most immediate implication of this result is that river diversions for the purpose of coastal and delta plain sediment management can retain nearly all – we estimate 75 to 100% – of the sediments supplied to them from the river if they are situated in an appropriate environment. The caveat that appropriate site selection is crucial to diversion performance is relevant in part because it aids the management community in selecting appropriate diversion analogs. This research shows that diversions to vegetated settings that are far removed from coastal processes are able to retain much more sediment than delta lobes that are exposed to open water wave and tide processes. Land building sediment diversions will take on increasing importance worldwide as rising relative sea levels transgress upon heavily populated deltaic coasts.

An interesting aspect of the analysis in Chapter 2, and of previous studies of the same region (Shen et al., 2015), is that crevassing is the primary driver of floodplain

aggradation proximal to the river. Not only that, but multiple crevasses are likely to operate simultaneously along delta distributary channels. I pick up this thread in **Chapter 3, "Flow Loss in Deltaic Distributary Networks"** which looks at the influence of widespread flow loss along delta distributaries, but this time from the perspective of the channels rather than that of the floodplain. The reach of a river where its hydraulic geometry adjusts to meet base level, usually referred to as the backwater reach, has been extensively studied in recent years as a region defined by spatial variation in flow and sediment transport conditions, and of intense morphologic activity in the bed. But most of the field data used to characterize this important region have been collected in intensively managed rivers that flow through populated areas, and are therefore prevented from losing flow to crevasses or overbanking. To address this disconnect we collected hydrodynamic data throughout the networks of three subdeltas in the Mississippi River's Birdsfoot Delta. The three channel networks are relatively unconfined, and allowed to lose flow overbank, and through numerous small cuts in the levees. This data set of linked hydrodynamic and water surface profile measurements collected simultaneously throughout three adjacent channel networks is unique. We use this data set to inform a set of numerical simulations of channel hydrodynamics in the backwater reach, which show that flow loss along the length of channels plays an important role in modulating flow and sediment transport in unmanaged channels. This observation is important to our understanding of distributary channel networks, and we use our model and field data to develop a metric of channel stability. Examining the data in light of the stability metric shows that flow loss plays a significant role in maintaining channel network stability. Our results imply that flow loss is important to channel bed response in the backwater reach,

potentially complicating how we interpret data from modern managed systems that are not allowed to lose flow.

The third project, **Chapter 4, "Sediment Storage Partitioning in Alluvial Stratigraphy: The Influence of Floods",** is motivated by the goals of interpreting environmental signals that are preserved in sedimentary deposits and predicting the geometry and connectedness of sediment bodies in the subsurface. Here we apply physical delta basin experiments to consider the influence that a river's hydrograph has on whether river-borne sediments are preferentially stored in channel or floodplain deposits. Our results are counterintuitive: For the parameter space we examine, we find that including floods in the input hydrograph actually decreases the proportion of floodplain deposits that is preserved in the resulting strata relative to a system with a constant discharge input. This change is the result of differential channel mobility in the two systems.

The topic of floods affecting sediment partition in alluvial plains has received relatively little attention, but there is evidence (e.g. Aalto et al., 2003) from modern systems that hydrograph character can play a significant role. This line of inquiry is important to practitioners in a variety of disciplines. The ratio of channel to floodplain deposition is an important input parameter for basin filling models of alluvial stratigraphy, and our results provide modelers with a better mechanism to link their inputs to climate driven processes than was previously available. Floodplains are also well known as sinks for fine grained sediments and for terrigenous carbon, and a better understanding of the sedimentary response to changing precipitation patterns will help researchers who seek to predict the influence of climate change on the global carbon

budget. We conclude by placing our study in the context of others that have examined the conditions under which information about floods are transferrable into the stratigraphic record, and describe how a researcher might use our results to select a study site to answer specific questions about climate or environmental signals.

2 Efficient retention of mud drives land building on the Mississippi Delta plain

Christopher R. Esposito, Zhixiong Shen, Torbjörn E. Törnqvist, Jonathan Marshak, Christopher White

2.1 Abstract

Many of the world's deltas – home to major population centers – are rapidly degrading due to reduced sediment supply, making these systems less resilient to increasing rates of relative sea-level rise. The Mississippi Delta faces some of the highest rates of wetland loss in the world. As a result, multi-billion dollar plans for coastal restoration by means of river diversions are currently nearing implementation. River diversions aim to bring sediment back to the presently sediment-starved delta plain. Within this context, sediment retention efficiency (*SRE*) is a critical parameter because it dictates the effectiveness of river diversions. Several recent studies have focused on land building along the open coast, showing *SRE*s ranging from 5 to 30%. Here we measure the *SRE* of a large relict crevasse splay in an inland, vegetated setting that serves as an appropriate model for river diversions. By comparing the mass fraction of sand in the splay deposit to the estimated sand fraction that entered it during its life cycle we find that this mud-dominated sediment body has an *SRE* of ≥75%, i.e., dramatically higher than its counterparts on the open coast. Our results show that transport pathways for mud are critical for delta evolution and that *SRE* is highly variable across a delta. We conclude that sediment diversions located in settings that are currently still vegetated are likely to be the most effective in mitigating land loss and providing long-term sustainability.

2.2 Introduction

Most large rivers do not transport sufficient sediment to the coast to fill the accommodation that will be created on their delta plains due to rapid 21st century sea-level rise (Giosan et al., 2014). This shortfall ensures a global retreat of deltaic coasts and presents an existential threat to some of the densest human populations, most valuable economic infrastructure, and most vibrant ecologies on Earth (Ericson et al., 2006; Giosan et al., 2014). To mitigate land loss, sediments can be distributed to vulnerable or otherwise important locations with controlled diversions of sediment-laden river water (Day et al., 2007; Kim et al., 2009; Paola et al., 2011; Giosan et al., 2013; Smith et al., 2015; Auerbach et al., 2015; Coastal Protection and Restoration Authority of Louisiana, 2017). The most effective techniques for such diversions are subject to debate (Blum and Roberts, 2009; Kim et al., 2009; Nittrouer and Viparelli, 2014a; Blum and Roberts, 2014; Nittrouer and Viparelli, 2014b), but it is clear that maximizing sediment retention efficiency (*SRE*) is a critical concern (Blum and Roberts, 2009; Paola et al., 2011). Because fine sediments are highly mobile in suspension and delta plains are often regarded as inefficient traps for mud (Giosan et al., 2014), much of the literature on diversions has focused on extracting sandy material from the trunk channel (Nittrouer et al., 2012a; Nittrouer and Viparelli, 2014b; Meselhe et al., 2016). However, mud comprises 80% or more of the incoming sediment load in most rivers (Giosan et al., 2014) and often dominates their delta-plain deposits.

Published estimates of SRE (Nittrouer et al., 1995; Allison et al., 1998; Goodbred and Kuehl, 1998; Törnqvist et al., 2007; Blum and Roberts, 2009; Day et al., 2016; Roberts et al., 2016) vary from 5 to 80%, a range that is too wide to be useful for

planning purposes, but which suggests that the specific depositional setting is an important control. Here we propose that vegetated inland settings that are protected from wave and tide energy can be highly efficient in trapping sediment, especially mud, and thus offer desirable locations for diversions that target mud for coastal restoration. We test this hypothesis by measuring the SRE of a large crevasse splay at an inland setting in the Mississippi Delta (MD), finding it to exceed 75%. This is substantially higher than estimates of SRE in the Wax Lake Delta (WLD), a well-studied prograding lobe at the coast of the (MD) (Figure 2-1a) that has is often used as a diversion analog. The WLD is sand-dominated (Roberts et al., 2003; Kim et al., 2009) and has been estimated to have an SRE ranging from 5 to 30% (Törnqvist et al., 2007; Kim et al., 2008; Roberts et al., 2016). Our results demonstrate the essential role that mud plays in vertically aggrading delta plains, and the contrast with the WLD highlights the importance of careful site selection for diversion projects.

We set this study in the Attakapas Crevasse Splay (ACS), a ~60 km^2 landform that was constructed from 1.2 to 0.6 ka (Shen et al., 2015) and initially discharged into a mature cypress swamp that is now preserved as a regionally continuous wood peat bed underlying overbank strata (Törnqvist et al., 2008) in the Lafourche subdelta of the MD (Figure 2-1). We choose a crevasse splay because such features are ubiquitous along all major distributary channels (Davis, 1993; Day et al., 2007). Their prominent expression in the MD attests to their role as fundamental delta building blocks (Figure 2-2, Figure DR2 in Shen et al., 2015). We chose this particular crevasse splay because of the well-established stratigraphy based on 132 cores and a chronology based on extensive ^{14}C and OSL dating in the region (Törnqvist et al., 1996; Shen et al., 2015), and because its size

and timescale of activity are in line with those of planned diversion projects in the MD (Coastal Protection and Restoration Authority of Louisiana, 2017).

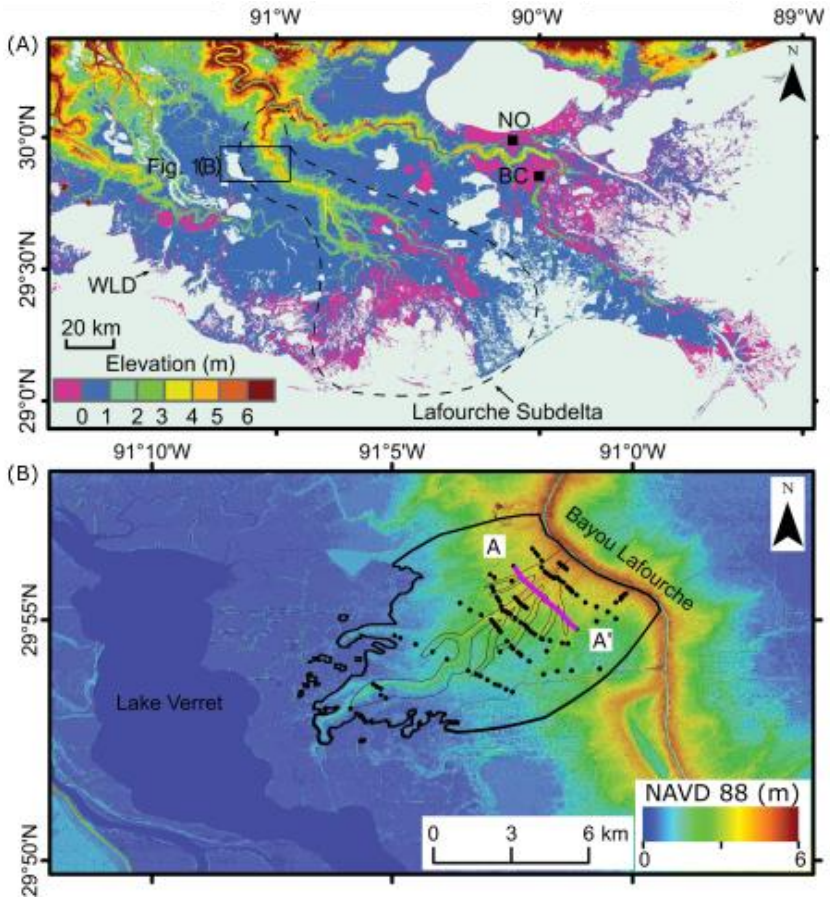

Figure 2-1. Digital elevation models (DEMs) of the study area.

(a) Mississippi Delta, Louisiana, USA. Regional data is derived from the 1/3 arc-second DEM of the US Geological Survey (http://viewer.nationalmap.gov/basic/#startUp), accessed in September, 2015. (b) The Attakapas Crevasse Splay at Napoleonville, Louisiana. Black dots mark core locations. The surface expression of the silty splay deposit used in the 3D model is marked by the thick black line. Thin black lines show alluvial ridges associated with splay channels. The local DEM is derived from Light Detection and Ranging data available from Atlas: The Louisiana State GIS (http://atlas.lsu.edu). NO—New Orleans; BC—Belle Chasse; WLD—Wax Lake Delta; NAVD 88—North American Vertical Datum of 1988.

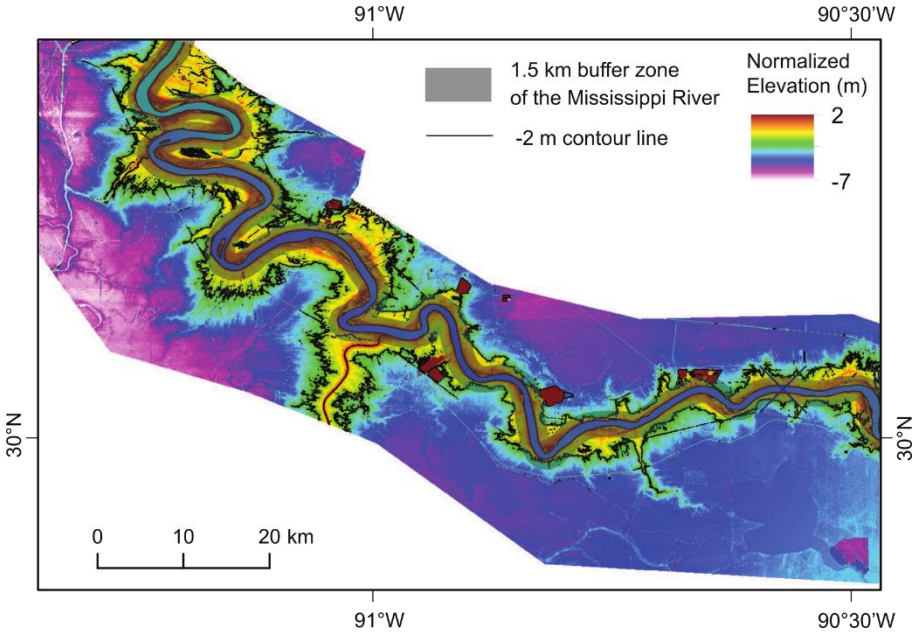

Figure 2-2. Crevasse Splays on the Mississippi River

Normalized DEM of the LMR between Baton Rouge and the Bonnet Carre Spillway, and the adjacent portion of the delta plain for crevasse splay identification. The DEM was obtained by subtracting a planar surface that best fits the Mississippi River natural levee long profile from the DEM of the studied reach. A -2 m contour of the normalized DEM and a 1.5 km buffer zone around the centreline of the MR are used to identify crevasse splays. The area where the -2 m contour lies outside the buffer zone is identified as formed by a crevasse splay (see Shen et al., 2015, for further explanation), which accounts for ~75% of the bank length in the studied reach. Note the reduction in the extent of crevasse splays downstream of the avulsion site; this is likely due to the fact that the duration of channel activity upstream of this point was considerably longer than in the downstream reach.

2.3 Measuring sediment retention efficiency

There are only a handful of studies that have attempted to tie the bulk sedimentary properties of a recent deposit to sediment-transport properties in the river that created it (Törnqvist et al., 2007; Kim et al., 2009; Giosan et al., 2013; Day et al., 2016), and we are unaware of any with a subsurface data set as rich as the one available for the ACS. While many workers have published on the "river side" issues concerning diversions, including the sediment available (Kesel, 1988; Blum and Roberts, 2009; Allison et al., 2012) and the physics of extracting sediment from the trunk channel (Allison and Meselhe, 2010; Nittrouer et al., 2012a; Meselhe et al., 2012; Allison et al., 2013), only recently have researchers begun to investigate "basin side" issues that impact *SRE* (Xu et al., 2016). The availability of detailed sediment-transport data from the modern Lower Mississippi River (LMR) (Allison et al., 2012) provides a unique opportunity to connect fluvial sediment budgets to the sediments preserved in the delta.

We estimate the *SRE* of the ACS with a 3D model (Figure 2-3) based on the 132 cores augmented by 53 grain-size analyses. These data are used to quantify the sand fraction (>62.5 μm) in the ACS deposit (S_d), and we estimate the sand fraction in the ACS input (S_i) from published hydraulic and sediment-load data from the modern LMR. If we compare the two sand fractions, and stipulate that 100% of the sand that enters the system is retained, *SRE* is obtained with Eq. 1:

$$SRE = \frac{S_i}{S_d} \quad (1)$$

This scheme measures the loss of mud (<62.5 μm) from the splay. When S_d is very close to S_i, *SRE* approaches 100%. Therefore, a deposit with a grain-size composition that closely resembles its input is an efficient sediment trap. In the MD, fed by a river whose current sediment load is ~80% mud, this means that sand-rich deposits are the products of ineffective sediment traps.

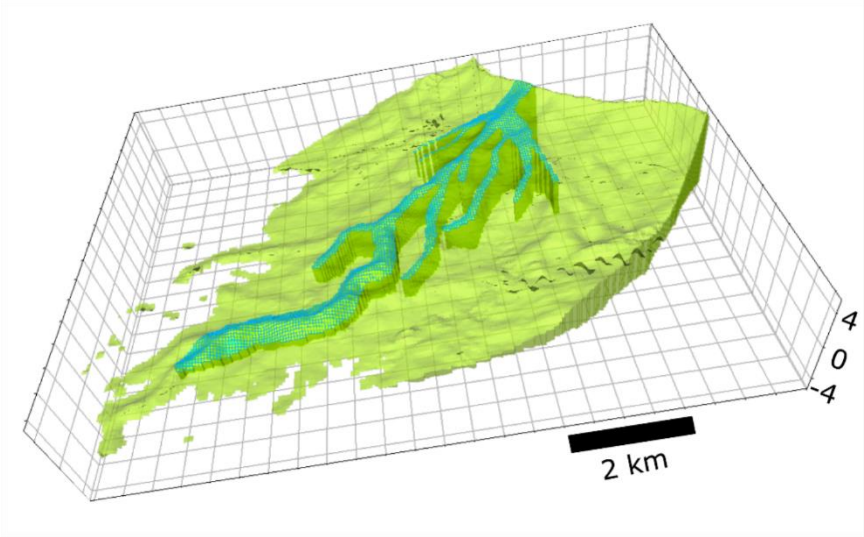

Figure 2-3. 3D geometry of the Attakapas Crevasse Splay.

Vertical axis is in meters relative to NAVD 88. The relatively sandy channel deposits are shown in blue green; light green refers to the silt-dominated portion of the splay. The transparent top bounding surface is the LiDAR-derived modern land surface, and the base is the clay to silt transition shown in Figure 2-4. Wherever possible, the lateral boundary is chosen to be the intersection of the top and basal bounding surfaces. On the lateral edges, where the deposit does not pinch out and these two surfaces do not meet, the boundary was chosen manually.

2.3.1 Sediment texture

All 132 cores were described in the field at 10 cm increments following the United States Department of Agriculture texture classification system (cf. Shen et al., 2015). Texture classes encountered were very fine sand (vfS), sandy loam (SL), silt loam (SiL), silty clay loam (SiCL), silty clay (SiC), and clay (C). Organic-rich clays are denoted as humic clay (HC). The sand fraction for each texture class was determined by grain-size analysis of 53 samples taken from three separate cores (Table 2-1). For our analysis we combined SL and vfS into a single class to which we applied the sand fraction measured for vfS samples. This is consistent with our objective to estimate an upper limit of sand content in the deposit. We combined SiC, HC, and C into a single class as well. Samples were treated with hydrochloric acid to remove carbonates and with hydrogen peroxide to remove organic matter, then wet sieved through a 106 μm screen. Both fractions were dried and weighed, then analyzed for grain size. The coarse fraction was analyzed with a Retsch Technology CAMSIZER and the fine fraction with a Horiba LA-300 Laser Particle Size Analyzer. The resulting sediment distributions were weighted and patched together to obtain a continuous curve that was used to determine the sand fraction.

Sediment Texture Class	mean sand fraction	2σ error	max sand	min sand	n	texture fraction, channel	texture fraction, non-channel
Very Fine Sand (vfS), Sandy Loam (SL)	0.2398	0.1463	0.3159	0.1106	23	0.17	0.11
Silt Loam (SiL)	0.0454	0.0396	0.0662	0.0253	6	0.32	0.23
Silty Clay Loam (SiCL)	0.0089	0.0294	0.0445	0.0000	10	0.40	0.46
Silty Clay (SiC) Clay (C) Humic Clay (HC)	0.0066	0.0066	0.0330	0.0000	14	0.11	0.20

Table 2-1. Sediment texture data used to calculate S_d.

Mean sand fraction, error, and min and max values obtained from 53 sediment samples of the texture classes present in the ACS. Texture fraction in channel/non-channel deposits is calculated from the number of texture descriptions from cores collected inside or outside of our channel boundary, not from interpretations such as that shown in the cross section in Figure 2-4. Weighting these data by the volumes of channel and non-channel deposits in the splay gives a total splay sand fraction of 0.045. Propagating the 2-σ errors yields a minimum splay sand fraction of 0.028 and a maximum of 0.062.

2.3.2 Crevasse splay 3D model and deposit sand fraction

All 3D modeling was done by means of Schlumberger's Petrel geomodeling software. The basal bounding surface of the ACS was generated with R, using the gstat package (Pebesma, 2004). The ACS consists of primarily muddy facies that overlie a wood peat bed that predates occupation of the region by the precursor of the modern LMR, Bayou Lafourche (Törnqvist et al., 1996). The earliest Lafourche deposits feature a 1-3 m thick clay bed that transitions abruptly into a silty matrix with sandy ribbons embedded within it (Figure 2-4). We interpret the clay to silt transition as the base of the ACS, and the coarser sandy deposits as splay channel deposits.

The top bounding surface of the splay is the modern land surface as measured by LiDAR. The picked subsurface elevation of the clay to silt transition was linearly regressed on the elevation of the local land surface ($R^2 = 0.58$). This regression yields a useful result because higher elevations are correlated with thicker deposits, which have differentially compacted the underlying strata (Törnqvist et al., 2008). We use the regression function to generate a surface for the transition, which we refine by kriging the residuals and adding the result back to the surface. Adding the kriged residuals ensures that the regression surface matches our core picks exactly, and exploits local excursions from the regression trend to improve the estimate based on nearby data points. Wherever possible, the edges of the ACS were taken to be the intersection between the top and basal surfaces. When the surfaces diverge due to the occurrence of neighboring splays, the edge was chosen manually based on the local topography.

Channel bodies in the ACS are identifiable both as narrow alluvial ridges and as coarser sediment bodies in the subsurface. All channel bodies were modeled to extend through the full thickness of the splay. This choice makes the channel bodies appear somewhat less sandy than they might be in reality, but also makes them larger; the end result is a slightly sandier estimate of S_d overall, which is a conservative choice that results in a lower SRE value.

We determined the average sand fraction for the channel and non-channel portions of the ACS separately (Table 2-1). A volume-weighted average of these sand fractions yields the estimate of overall S_d for the ACS.

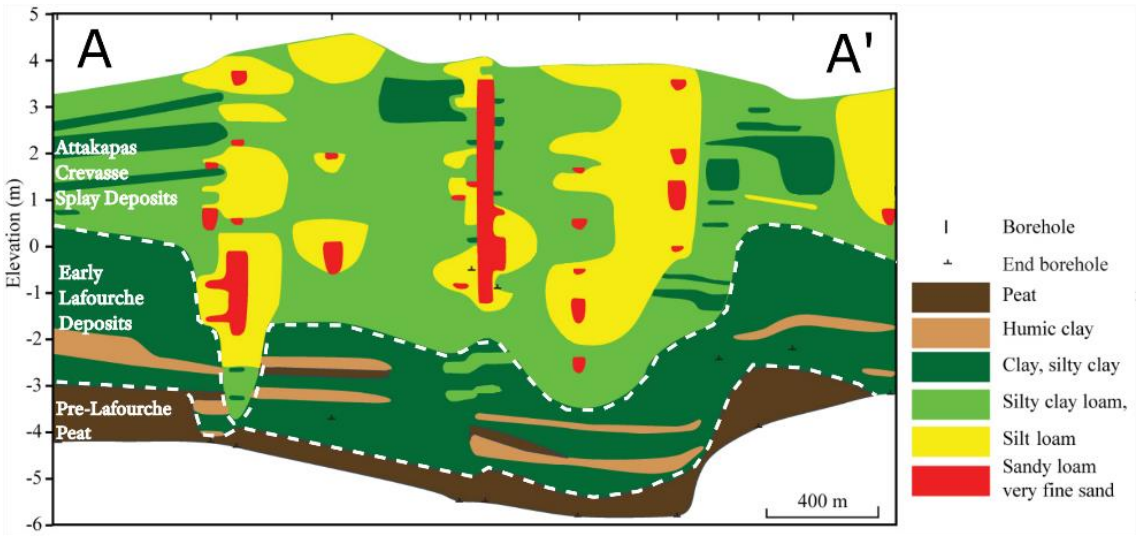

Figure 2-4. Stratigraphic cross section of the Attakapas Crevasse Splay.

The cross section along transect A to A′ (see Figure 2-1 for location), adapted from Shen et al. (Shen et al., 2015). Our 3D model (Figure 2-3) considers only sediments preserved above the clay to silty clay loam transition. Channel bodies can be seen as deposits of coarser material, often corresponding with alluvial ridges.

2.3.3 Input sand fraction

We estimated the yearly averaged sand fraction input into a 5 m deep crevasse channel emanating from a 30 m deep trunk channel. We obtained the depth of the trunk channel, Bayou Lafourche, from previous investigations of the region (Fisk, 1952). Shen et al. (2015) showed that the ACS deposit has a total thickness of up to 10 m, that the ACS was active during two episodes of rapid aggradation, and that similar thicknesses accumulated near the inlet during each episode. In keeping with these data, we used 5 m as a representative estimate of the depth of the primary crevasse splay feeder channel during its lifetime. This value is similar to that of other well-studied crevasse systems in the MD (Farrell, 1987). The flow depth of the trunk channel was assumed not to vary significantly, consistent with measurements in the modern LMR where at 100 km from the shoreline the flow depth varies less than 2 m throughout the year (Nittrouer et al., 2012b).

To estimate the input sand fraction (S_i), we used modern suspended sediment measurements from the United States Geological Survey gauge station at Belle Chasse, Louisiana ("BC" in Figure 2-1a) and published estimates of the sediment composition and hydraulic properties in the modern LMR (Nittrouer et al., 2012b; Ramirez and Allison, 2013). We divided river discharge into five bins, each of which was treated separately (Table 2-2) to estimate the channel width integrated concentration of sand and mud in suspension in the uppermost 5 m of the 30 m deep trunk channel. We then used rating curves (Allison et al., in review) to compute the discharge of suspended sediments corresponding to each daily water discharge. The lowest flow bin is assumed to carry

mud but no sand, consistent with modern observations (Nittrouer et al., 2008). Binning the data by water discharge reduces the influence of hysteresis on the sediment load. To obtain the sand fraction in the uppermost 5 m of the water column we used 1) a vertical profile of relative suspended sediment concentration for mud and sand in each discharge bin, 2) the total suspended load for each sediment class and discharge bin (estimated from gauge measurements at Belle Chasse), and 3) log-law velocity profiles for each discharge bin. All calculations can be seen in the 'Si' tab of the supplemental spreadsheet. Sand concentration is assumed to follow a Rouse profile (Rouse, 1936), while mud is well mixed. We use shear velocities in the range of published modern LMR measurements (Nittrouer et al., 2012b; Ramirez and Allison, 2013) when calculating Rouse and velocity profiles.

We assumed that the sand load obtained from Belle Chasse was composed of 125 μm and 250 μm grains, in a 35/65 split, consistent with measurements in the modern LMR (Ramirez and Allison, 2013). We calculated Rouse profiles for each sand fraction separately, and then added them together in proportion to obtain the concentration profile for suspended sand.

We adapted methods used in recent work in the modern LMR (Nittrouer et al., 2011) and the Rouse equation to calculate profiles of relative concentrations of suspended sand. The equation for relative concentration of suspended sand is:

$$\frac{r_n}{1-r_n} = [\left(\frac{H-Z}{Z}\right) - (\frac{z_a}{H-z_a})]^p \quad (2)$$

where r_n represents the relative concentration of sand in suspension in depth layer *n*, and is a function of channel depth (*H)*, height above the bed (*Z)*, thickness of the bedload

transport layer (z_a, which here is on the order of 10^{-4} m), and the Rouse number $p = \frac{w_s}{\kappa u_*}$. To calculate the Rouse number we use the Dietrich method (Dietrich, 1982) to determine sediment fall velocity (w_s), and take literature values for shear velocity (u^*) (Nittrouer et al., 2012b; Ramirez and Allison, 2013) and von Karman's constant κ.

Our Rouse profiles are not calculated using a near-bed reference concentration, and thus they describe the shape of the sand concentration profile but not its magnitude. We use these curves to define a set of proportionality constants k_n, that relate the relative concentration values, r_n, to the bottom value, r_1.

$$r_n = k_n r_1 \tag{3}$$

We then note that

$$Q_s = \sum v_n c_n \tag{4}$$

where Q_s is the channel integrated suspended sediment load for the size class in question, v_n is the velocity in vertical layer n, and c_n is the width-integrated sediment concentration in the same layer. For simplicity, we show the case where each layer is of unit thickness and is the full width of the channel. The width of the channel will affect the magnitude of the concentration values, but will not affect the suspended sand fraction, which is the objective of the computation.

Using the proportionality constants defined in Eq. (3) we now expand Eq. (4) and obtain a value for c_1.

$$Q_s = v_1(k_1c_1) + v_2(k_2c_1) + \cdots + v_n(k_nc_1) \quad (5)$$

$$c_1 = \frac{Q_s}{\sum_1^N v_n k_n} \quad (6)$$

The remaining c_n values can be obtained by multiplying c_1 by the appropriate k_n.

Note that we have calculated the width-integrated sand concentration in our depth interval rather than the sediment load. We do this because crevasse splays can distort local flow fields, but concentrations in a turbulent flow can be inherited from upstream. To calculate the sand fraction entering the ACS we assume that the splay takes a constant fraction of the trunk channel's discharge throughout the hydrograph, which we call γ. This assumption finds support in data from the West Bay, Baptiste Collette, and Grand Pass crevasses in the birdfoot delta of the modern LMR (Allison et al., 2012).

The sand fraction delivered to the ACS, S_i, is then calculated as

$$S_i = \frac{\sum_j c_{sand,j}\gamma Q_{w,j}}{\sum_j c_{sand,j}\gamma Q_{w,j} + \sum_j c_{mud,j}\gamma Q_{w,j}} \quad (7)$$

where $c_{sand,j}$ and $c_{mud,j}$ are average concentrations in the uppermost 5 meters for discharge bin j, and $Q_{w,,j}$ is the water discharge in the trunk channel at each bin integrated through the entire Belle Chasse record. We make no assumptions about γ other than that it is nonzero. The value of γ does not affect the result of this calculation.

River Inputs	bin discharge range ($m^3 s^{-1}$)	<15000	15000-20000	20000-25000	25000-30000	>30000
	average discharge in bin ($m^3 s^{-1}$)	9658	17417	22449	27045	30959
	days spent at this bin (Oct 1 1989 - Sept 30 2013)	5116	1302	1559	673	116
	total water discharge during record ($m^3 s^{-1}$)	4.27E+12	1.96E+12	3.02E+12	1.57E+12	3.10E+11
	Total sediment discharge during record (metric tons)	4.98E+06	4.28E+06	7.06E+06	3.69E+06	7.13E+05
	average sand load, full channel (kg s^{-1})	34	453	965	1563	2168
	average mud load, full channel (kg s^{-1})	940	2833	3563	3914	3983
	sand fraction of total suspended load (-)	0.03	0.14	0.21	0.29	0.35
Hydraulic Parameters	u^* estimate (m s^{-1})	0.06	0.06	0.06	0.09	0.09
	z_0 (m)	0.0005	0.0005	0.0005	0.0005	0.0005
Top 5 m	average sand concentration per unit width, top 5 m (kg m^{-2})	0.00	2.60	5.53	9.05	12.55
	average mud concentration per unit width, top 5 m (kg m^{-2})	21.02	63.33	79.65	58.33	59.35
	average sand fraction (S_i), top 5 m (-)	0.00	0.04	0.06	0.13	0.17

Table 2-2. Data used to calculate S_i.

The sand and mud concentrations for each bin are weighted with the respective total water discharge to provide a yearly average sand fraction input to the splay of 0.066.

2.4 Results

The 3D model (Figure 2-3) shows a half-lens shaped deposit with a maximum thickness of ~10 m where flow entered from Bayou Lafourche. The total volume of the ACS is 1.62×10^8 m^3. Former channels can be identified as topographic ridges (Figure 2-1b) that correspond with sandier ribbons in the subsurface (Figure 2-4). While the narrow alluvial ridges associated with crevasse channels are the most striking topographic features on the splay, channel deposits constitute only 15.6% of the ACS deposit. Sandy textures (sandy loam, very fine sand) make up 17% of the channel bodies, but only 11% of the non-channel deposits. On the scale of the entire ACS, silty textures (silt loam, silty clay loam) are by far the most common. Texture descriptions were calibrated to sand fraction by grain-size analysis of the 53 samples (Table 2-1). The results of this analysis show that the fraction of sediment mass in the ACS that is represented by sand-sized grains is 0.045±0.017. We use the mean value as our estimate of S_d when calculating *SRE*.

Using modern suspended sediment data we estimate that the yearly averaged input sand fraction (S_i) is 0.066 (Table 2-2). Combined with the estimated ACS sand fraction (S_d) of 0.045 (Table 2-1), we obtain a *SRE* value that exceeds 100%. This value is likely the result of the historical decline in sediment load documented in the modern LMR which is treated more fully below.

2.5 Discussion

2.5.1 Uncertainty in estimating *SRE*

The ACS boundary is defined by the extent of silt-dominated deposits and therefore includes all sandy sediment bodies encased within it. Any reasonable splay boundary will exclude the most mobile sediments, so we proceed with the understanding that some fine sediments were lost to the surrounding environment. For example, the bank of Lake Verret near the downstream end of the ACS is convex where splay-derived sediments have partially filled it (Figure 2-1b), suggesting a loss of fine sediments across our defined boundary.

Unlike S_d, we are unable to measure S_i directly, so we apply modern sediment-load measurements to the prehistoric channel geometry to estimate the sand fraction that was discharged to the ACS. The Lafourche channel had a depth similar to the modern LMR channel downstream of Belle Chasse (Fisk, 1952), which gives us confidence to apply modern hydraulic parameters in our analysis. We do not consider the effect of channel planform on the cross-channel distribution of sediments.

Spillways that are part of the modern flood-control system prevent the largest floods, which had magnitudes substantially greater than what is allowed today (Barry, 1998). The discharges in our largest bin (>30,000 $m^3 s^{-1}$) carry only 3% of the average yearly suspended sediment load, implying that these large magnitude events probably occurred infrequently enough that their impact on the crevasse sediment budget was small. The omission of larger but even less frequent floods would have even less of an

effect. To the extent that this omission is important it means that the value for S_i, and therefore *SRE*, is underestimated.

Perhaps the largest uncertainty is the sand and mud fraction carried by the LMR prior to human modifications. It is well documented that the suspended sediment load of the modern LMR was dramatically reduced by dams in the mid-20th century (Kesel, 1988), but because it is likely that pre-dam sediment loads were elevated due to widespread agricultural activity in the drainage basin (Keown et al., 1986; Tweel and Turner, 2012), it is difficult to estimate the suspended sediment loads that prevailed from 1.2 to 0.6 ka. Recent modeling results suggest that the suspended sand load delivered to the MD is buffered from upstream change for timescales on the order of 1000 years (Nittrouer and Viparelli, 2014b). With that in mind, the events that may have substantially changed the suspended sand load are either so recent (dams in the tributaries, rapid deforestation associated with expanding agriculture; <200 years ago) or so long past (glacial outwash floods; >10,000 years ago (Rittenour et al., 2007) that it is reasonable to apply modern sand loads to the Lafourche channel.

The question of paleo-mud loads is more challenging, as there is no accepted estimate for the magnitude of the sediment load increase due to expanding agriculture. Instead of choosing one particular mud load (and implied sand fraction) we performed our S_i and *SRE* calculations for a range of possibilities. Assuming that the modern mud load reflects a 30% reduction from the prehistoric condition leads to an *SRE* value of approximately 100%, thereby imposing a lower limit on mud load reduction. A 50% reduction in mud load, which is consistent with the limited data that are available for the LMR prior to widespread intensive agriculture (Tweel and Turner, 2012), corresponds to

an *SRE* of 75%. We therefore estimate that the ACS had an *SRE* value between 75 and 100%, which corresponds to a 30 to 50% reduction in suspended mud load. It is important to note that the conservative assumptions that underpin our estimates of S_i and S_d make 75% a conservative lower bound on *SRE*.

We performed independent sensitivity analyses on our estimates of S_d and S_i. For S_d we varied the fraction of the deposit composed of channel bodies from 0.1 to 0.4, and obtained S_d estimates of 0.044 and 0.048, respectively. Our best estimate of the channel-deposit fraction (0.16) was used for our calculations, leading to our base S_d estimate of 0.045 (Figure 2-3, Table 1). For S_i we varied the hydraulic, sediment composition, and channel geometry parameters used in our estimate over reasonable ranges, and found that our estimate is most sensitive to the depth of the crevasse inlet. Increasing the inlet depth to 10 m or decreasing it to 3 m would result in *Si* values of 0.10 and 0.04, respectively. We do not have sufficient control over the S_i parameters to define a probability distribution for *SRE*, but our sensitivity analysis supports the claim that our choices are conservative in that they result in lower bounds for S_i and *SRE*. All sensitivity testing calculations are shown in the supplemental spreadsheet.

2.5.2 Implications for delta evolution and sustainability

The ACS is overwhelmingly composed of mud, with sand-sized grains accounting for only ~5% of its mass. This indicates a system that is highly efficient in retaining fine-grained sediments. Regional analyses of delta-plain topography (Figure 2-4; and Figure DR2 by Shen et al. (2015)) show that crevasse-splay deposits are the dominant building blocks of the proximal overbank environment, and that the ACS is one of the largest

splays in the region. With its well-developed channel network, the ACS likely drew more water, from greater depths, than other crevasse splays along Bayou Lafourche, and is therefore likely to be comparatively enriched in sand. Because of this, and because some fine material must have been lost beyond our downstream boundary, our estimate of S_d likely resides near the upper limit for crevasse splays in the MD.

The ~5% sand fraction found in the ACS stands in contrast to the much higher values observed in prograding coastal delta lobes such as the WLD, where the sand fraction might be as high as 50%. A value of 67% sand for the WLD has been used (Törnqvist et al., 2007; Nittrouer and Viparelli, 2014a), though that value implicitly assumes that the sandy deposits documented in the WLD stratigraphy (Roberts, 1997; Roberts et al., 2003) are composed entirely of sand. Applying a mean sand content of 70% to the WLD sandy deposits (well above the highest sand content that we have observed in our study area; Table 1) implies a total sand content of 47%, although substantial work will be needed to confirm this. What is clear though is that the sand fraction of the WLD is an order of magnitude greater than that of the ACS for a similar input, indicating a much lower *SRE*. The implication is that *SRE* varies considerably depending on the specific depositional setting, a finding that we expect to apply in most large deltas.

Recent researchers have given considerable attention to the importance of coarse-grained sediment as a restoration tool (Nittrouer et al., 2012a; Nittrouer and Viparelli, 2014b), but proximal overbank deposits in the Mississippi Delta are dominantly composed of mud (e.g., McFarlan, 1961; Frazier, 1967; Törnqvist et al., 1996). Our results highlight the utility of the more plentiful mud load. While significant land loss in

the Mississippi Delta is inevitable, accretion rates that persisted in the mud-dominated ACS for centuries (1–4 cm yr-1; Shen et al., 2015) may locally be sufficient to keep up with present-day rates of relative sea-level rise in the MD (1.3 ± 0.9 cm yr-1) (Jankowski et al., 2017) even after accounting for enhanced compaction due to sediment loading (Törnqvist et al., 2008). The goal of river diversions is to maximize their land building potential, which is determined by both sediment supply and *SRE*. Coarse-grained sediment is largely deposited on the delta front where the *SRE* tends to be low. As a result, land building with coarse-grained sediment needs a very large sediment input, which implies designing relatively deep diversion channels to extract the coarse grains that are more abundant deeper in the water column (Meselhe et al., 2012). Consequently, only a few such projects can be operated at any given time and the mud load is mostly lost. Contrary to the viewpoint that only coarse sediment builds land (Nittrouer and Viparelli, 2014b), we find a deltaic feature that is almost entirely fine-grained but still sufficiently elevated to support agriculture 9 km from the trunk channel, 600 years after its final depositional episode. The high *SRE* values measured here point to inland crevasse splays as more appropriate restoration models than prograding coastal delta lobes.

The LMR discharge was shared between Bayou Lafourche and the modern LMR when the ACS was active (cf. Törnqvist et al., 1996). Since the partitioning of the discharge between these two distributaries is unknown, we assume a roughly equal proportion of the sand and mud load. This is relevant because the ACS built a splay with an area comparable to the WLD even when the discharge was split between Bayou Lafourche and the LMR. The abundance of mud-dominated crevasse splays in the MD

shows the importance of mud pathways to delta evolution. Their large numbers (Figure 2-2) also make it conceivable that numerous crevasse splays were active at any given time, thus highlighting their potential as land builders compared to a single, terminal delta lobe such as the WLD.

Our results have implications for sediment management strategies in the MD. A significant portion of the vegetated delta plain is within ~1 m of sea level (Figure 2-1a) and will likely submerge by the end of the century if its elevation is not increased (Blum and Roberts, 2009; Coastal Protection and Restoration Authority of Louisiana, 2017). River diversions can exploit high *SRE* values in these environments to maximize gains from the limited sediment load of the modern LMR, and can promote vertical land growth rapidly enough to locally keep up with relative sea-level rise. By contrast, diversions near the open coast are exposed to waves, tides, and currents, reducing their SRE and making their long-term viability questionable (Blum and Roberts, 2009). Considering the enormous costs of these projects (Coastal Protection and Restoration Authority of Louisiana, 2017), focusing resources on diversions in emergent settings that are still vegetated is preferable. These issues are not unique to the MD (Ericson et al., 2006; Giosan et al., 2013, 2014; Auerbach et al., 2015), but the political and economic ability to construct system-scale river management infrastructure is not yet present in most other large deltas. We expect this to change as the sea encroaches on major population centers worldwide. Therefore, the lessons learned from such novel attempts to divert sediment back to the delta plain in the MD have the potential to be impactful globally.

2.6 Conclusions

The late Holocene stratigraphic record of the Mississippi Delta shows that crevasse-splay deposits consist of ~95% mud. The sediment retention efficiency in crevasse splays that form in vegetated environments, sheltered from waves, tides, and coastal currents, exceeds 75% and may well approach 100%. This is dramatically higher than rates observed in prograding coastal delta lobes, which retain 5 to 30% of the incoming sediment. This contrast highlights the variability in retention rates among different portions of a single delta, and points to the importance of mud pathways for delta evolution. While large volumes of sand are associated with land building in open water, accretion rates of mud alone can be sufficient to locally match relative sea-level rise in a vegetated environment that is isolated from marine processes. It is important that planning efforts for coastal restoration projects incorporate land building models that account for the high spatial variability in *SRE* on deltas. Coastal managers can site river diversions to take advantage of locally high sediment retention efficiency by choosing locations that a) are protected from marine processes, b) contain existing emergent land with established vegetation, and c) are not at risk of imminent submergence. Such sites are likely to be more successful than those on the open coast.

2.7 APPENDIX

This chapter has been published in the journal Earth Surface Dynamics (Esposito et al., 2017). The data used in this paper, calculations, and sensitivity testing on important parameters can be found in the supplemental spreadsheet for that publication, available at https://doi.org/10.5194/esurf-2017-5.

Esposito, C. R., Shen, Z., Törnqvist, T. E., Marshak, J. and White, C.: Efficient retention of mud drives land building on the Mississippi Delta plain, Earth Surf. Dynam. , 1–11, doi:10.5194/esurf-2017-5, 2017.

3 Flow Loss in Deltaic Distributary Networks

Christopher Esposito, Ioannis Y. Georgiou, Kyle M. Straub

3.1 Abstract

The processes that influence flow and sediment dynamics in the lower reaches of large alluvial rivers have been intensively documented. But the trunk channel is often connected to the receiving basin by a network of terminal distributary channels, through which flow and sediment routing is not well understood. Maintaining navigation and flow through these channels is a critical management concern as sea level rises. In the Mississippi River Delta, the terminal distributary channels are not as intensively managed as the trunk channel, and are thus subject to flow loss along their length. This makes it difficult to apply the lessons learned from the trunk channel directly to the terminal distributaries. We present hydraulic measurements from three terminal distributary channel networks in the Mississippi River's birdfoot delta where lateral flow loss is widespread during flood conditions. To explore the effects of flow loss in the channels, we model gradually varied flow using 1-D equations which have been altered to account for mass and momentum loss through overbank flow and small lateral cuts in the levee. Our model results, which are validated against field observations, imply that the extent of flow loss is a geomorphic adjustment that acts to keep the along-channel trends in velocity and sediment transport similar throughout each channel network. We then apply the model to a hypothetical river with similar dimensions to the Mississippi River in order to explore the influence that the modern flood control system exerts on the morphological evolution of the channel bed. We find that preventing floodwater from leaving the trunk channel has probably deepened the channel in the lower portions of the backwater reach, but caused only small changes upstream.

3.2 Introduction

An influential body of literature documents hydraulic geometry gradients in the lower reaches of rivers where channel long profiles adjusts to meet receiving basins near shorelines (Nittrouer et al., 2012b; Wright and Parker, 2005a). The region of adjustment, often called the “backwater reach”, is characterized by sediment transport regimes that vary systematically with along-stream distance, making it a hotspot of morphological activity (Wright and Parker, 2005b; Jerolmack and Swenson, 2007; Nittrouer et al., 2011a, 2012b). In the Lower Mississippi River (LMR), where discharge records, bathymetric surveys, and sediment sampling are particularly robust, Nittrouer et al. (2012b) demonstrate that the streamwise trend in hydraulic geometry changes with flow discharge, suggesting the possibility of a complex response in the bed. At flood, river stage increases upstream but is held nearly constant by base level downstream, leading to a streamwise decrease in cross sectional area, thus a streamwise increase in velocity, and bed scour towards the shoreline. At low flow the trend is reversed; low stage upstream causes cross sectional area to increase with distance downstream, and the resulting streamwise decrease in velocity causes deposition. In this framework the bed morphology of the modern Lower Mississippi River is to a large extent set by the balance between these two competing states: Towards the shoreline, scour during floods outpaces deposition during low water, but further upstream the riverbed aggrades as flood scour is insufficient to flush sediments that have settled throughout the year.

This body of work presents a coherent picture of regional-scale sediment transport in the modern Lower Mississippi River, a channel that is confined by an engineered flood protection system, and which loses very little flow throughout most of its backwater

reach (Allison et al., 2012) except at specific, controlled locations. But flow loss is ubiquitous in unmanaged fluvial systems, so the confinement of the LMR channel complicates the task of applying the lessons learned to other locations or to the stratigraphic record. The same geometric constraint that necessitates channel deepening during floods could be satisfied by reducing the volume of water that flows through the channel were that permitted, and it is not clear under which conditions an unmanaged river would become deeper, become wider, or would lose flow.

The widely used term “bankfull flow” implies a frequency of overbanking events that points to their importance, and researchers interested in overbank dynamics have for decades studied flow paths exiting the main channels as important conduits for riverborne sediments (Smith et al., 1989; Slingerland and Smith, 2004; Rowland and Dietrich, 2005; Day et al., 2008; Shen et al., 2015). Likewise, substantial effort has been devoted to studying the in-channel effects of individual flow offtakes for channel maintenance and navigation, as well as for wetlands restoration and sediment management (Nittrouer et al., 2012a; Allison et al., 2013; Meselhe et al., 2016; Viparelli et al., 2015). But there is evidence that unmanaged fluvial channels lose flow over a large number of relatively small extractions (Humphreys and Abbot, 1867, Shen et al., 2015; Lewin et al., 2016). Shen et al. (2015, Fig DR2) examined a 55 km reach of Bayou Lafourche, which was once a major distributary of the Mississippi River, and found that 85% of the bank length was occupied by crevasse splays. These splays varied in size and alternated in their periods of activity, but their widespread presence shows that flow losses were integral to the function of the channel. Records of crevassing along the Lower Mississippi River before a comprehensive levee system was in place (Humphreys and Abbot, 1867) support

this. Our study investigates the response of river channels in the backwater reach to continuous flow loss along their length.

3.3 Field Setting

Our field data comes from the channel networks of three subdeltas in the Mississippi River's Birdsfoot Delta (Figure 3-1). Cubit's Gap, the largest of the three, formed in 1862, 5 km above Head of Passes on the East Bank (Welder, 1959). Baptiste Collette, 19 km above Head of Passes on the East Bank, is present as an inconsequential bayou on maps as early as the 1880's (Mississippi River Commission, 1885), but did not begin to expand until near the turn of the last century. Its entrance was closed with sheet piles from 1908 to 1915, and has remained open since the barricade was undermined in 1915 (E. J Dent, 1921). The Jump, nearly opposite Baptiste Collette on the West Bank, is 17 km above Head of Passes. It was formed by a crevasse in 1839. The distances from the riverbank to the Gulf of Mexico shoreline ranged from 100 to 500 m prior to the crevassing events.

Baptiste Collette (BC) and Cubit's Gap (CG) each have one dominant channel, while the two distributaries of The Jump (GT) are nearly equal in size and discharge. (Figure 3-2) We present data from two channels in each network, and refer to the Mississippi River as the "trunk channel" from which all three subdelta networks emanate. Flow is lost along all subdelta channels by overbanking and through small cuts in the levees. The cuts, some of which are natural and some of which are not, are typically on the order of 0.5 m deep (Boyer et al., 1997), and oriented nearly perpendicular to the main channel axis. Such cuts have been present throughout the history of the channel networks, though manmade features are more abundant now than prior to the middle of

the 20th century (The Coast And Geodetic Survey, 1906; U.S. Department of Commerce, 1965). Historical navigation charts show that the channel patterns in place today, including the relative widths of the channels, have persisted throughout the life span of each subdelta (Figure 3-3). In Cubit's Gap, where the early survey data is particularly good, we can see that the dominant channel was permanently established within the first 6 years of activity, and the secondary channel was in place within a decade. Bifurcation nodes, once established, are stable within ~200 m.

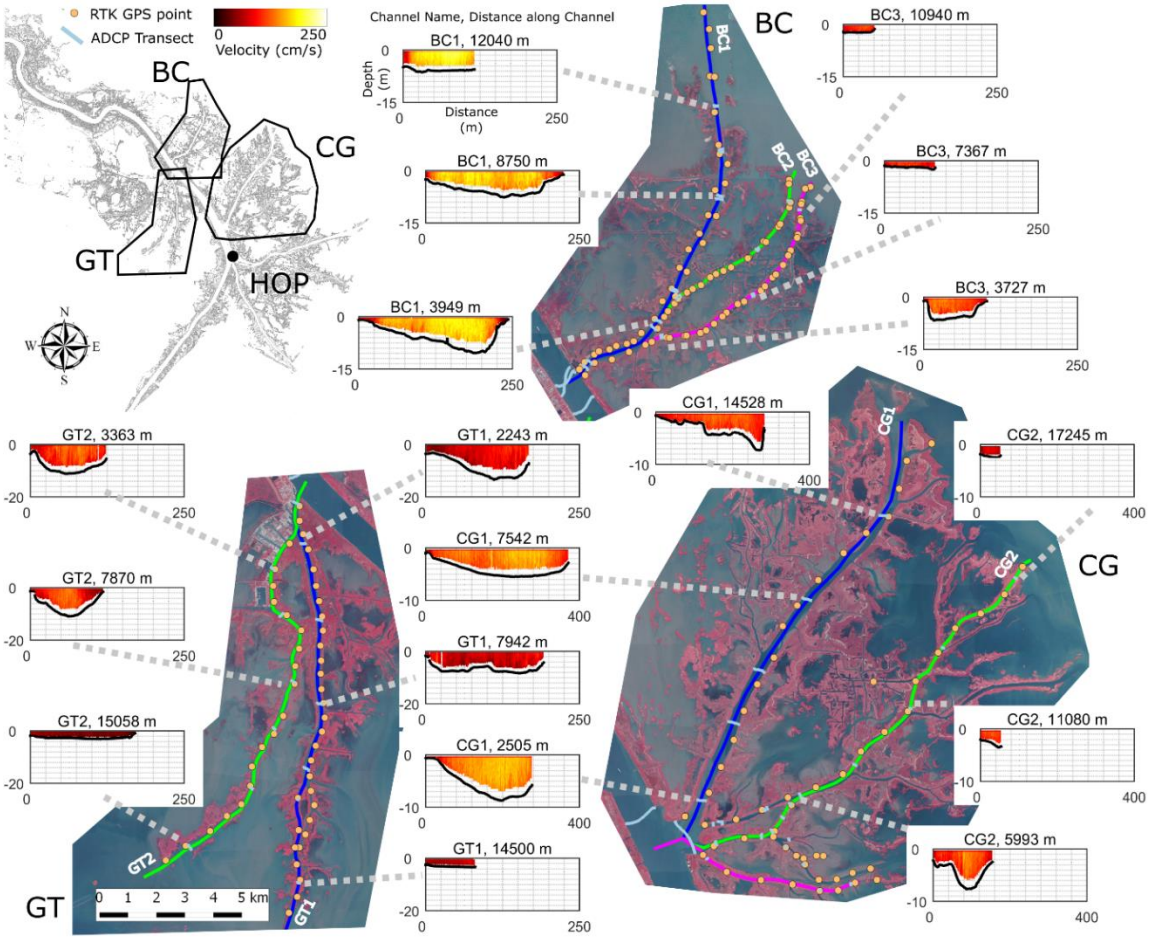

Figure 3-1. Overview map of study sites in the Mississippi River Birdsfoot Delta.

Overview map showing GPS points, ADCP transect locations, and ADCP transect data. Note that the horizontal and vertical scales of the ADCP transects are consistent for each channel, but not between channels. The ADCP transect at top, center of the figure serves as a key. Aerial imagery was downloaded from Louisiana's online GIS repository, Atlas. (Atlas: The Louisiana State GIS, 2003) BC: Baptiste Collette, CG: Cubit's Gap, GT: The Jump, HOP: Head of Passes.

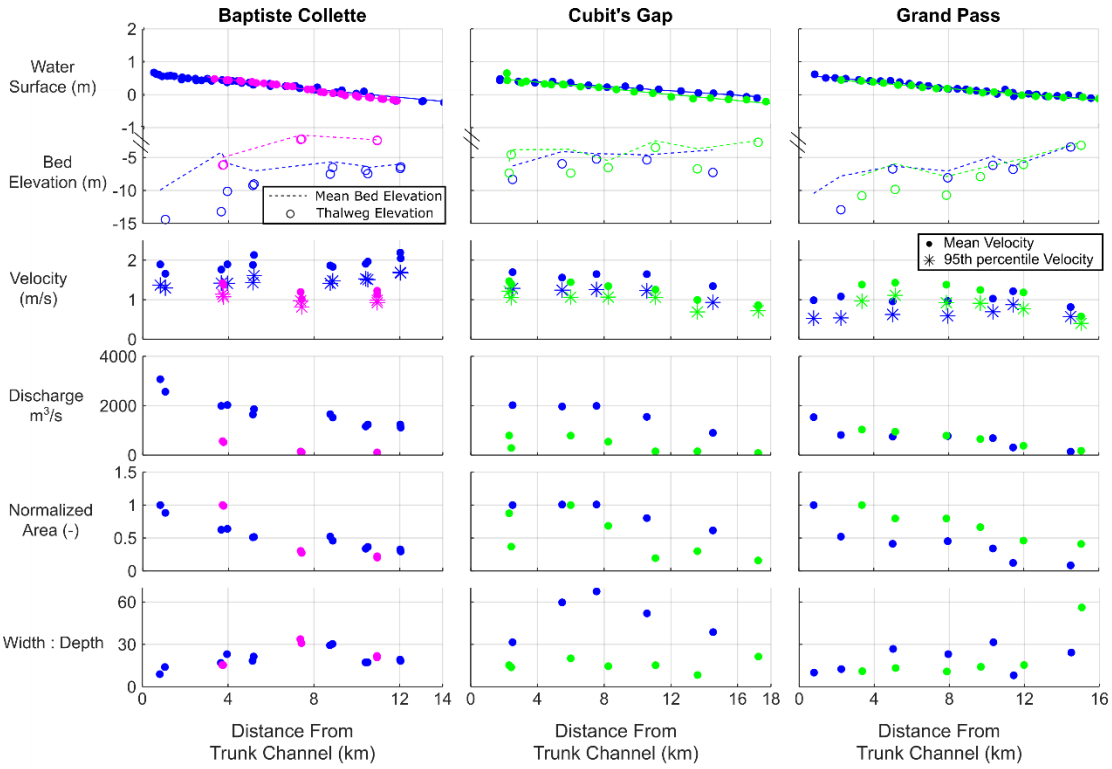

Figure 3-2. Field Data from Channel Networks

Colors correspond to the colors of channels shown in Figure 1. All elevations are displayed in NAVD88. Baptiste Collette was surveyed on March 31st (tide range ~6 cm), and again on April 3rd (tide range <2 cm) with only very small changes in the measured hydraulic properties. Data from both surveys is included here. The top row shows the water surface elevation and thalweg elevation. Note the change in vertical scale at -1 m. All subsequent rows show data that was derived from ADCP measurements. Note that area is displayed normalized by the inlet area. The CG2 channel has two inlets. Data from both inlets is plotted here separately. Combined values are shown in Table 2-1.

3.3.1 Anthropogenic Modifications

The passes studied here and the trunk channel have all been modified or maintained to varying degrees in order to facilitate navigation. A comprehensive treatment of the modifications since 1960 is given by (Sharp et al., 2013), and summarized here. The Mississippi River trunk channel was deepened in 1987 to include a 13.7 meter deep, 229 meter wide navigation channel, and regular maintenance dredging is required to maintain this channel downstream of Cubit's Gap. Additionally, the West Bay Sediment Diversion was completed in 2003 at River Kilometer 7.5 opposite Cubit's Gap. Opening West Bay induced sedimentation in the trunk channel that led to increased dredge activity beginning in 2006. The banks on both sides of the trunk channel are stabilized with revetments, which prevents widespread overbank flow and maintains the entrance widths and locations of the passes studied here. Baptiste Collette's main pass (BC1) and Grand Pass (GT1) were both dredged in 1978-1979, and flow constricting jetties were installed at the end of BC1. A sill, consisting of a woven willow mat weighted with rocks, was installed in Cubit's Gap in 1908 (Welder, 1959), and may still be limiting the entrance depths of CG1 and the north fork of CG2.

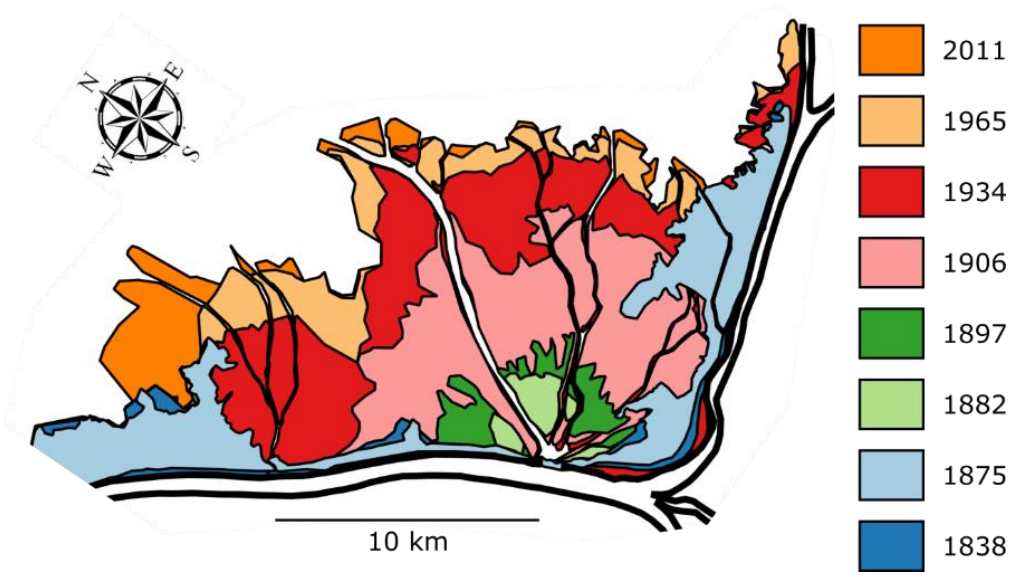

Figure 3-3. Land area growth of Baptiste Collette and Cubit's Gap

Land area growth of Baptiste Collette and Cubit's Gap subdeltas on the Mississippi River's East Bank. Internally ponded areas are not shown here. Historical maps were downloaded from NOAA's Historical Chart and Map Collection (http://www.nauticalcharts.noaa.gov/csdl/ctp/abstract.htm), and were digitized and georeferenced using QGIS.

3.4 Data Collection

Our primary field data set consists of water surface elevations collected with a survey grade GPS system linked to flow and channel geometry data collected with a boat mounted ADCP. The GPS and ADCP surveys were performed from March 31st through April 3rd, 2015, during which time the discharge in the Mississippi River measured at Belle Chasse (River Kilometer 120) ranged from 27,000 $\frac{m^3}{s}$ to 31,000 $\frac{m^3}{s}$. The maximum discharge allowed to pass Belle Chasse is 34,000 $\frac{m^3}{s}$, with excess flow diverted upstream at the Bonnet Carre Spillway (River Kilometer 205). Losses at Fort St. Philip (RK 31) remove approximately 7% of the discharge that passes Belle Chasse (Allison et al., 2012). ADCP and GPS data were always collected in the same channel network on a given day, and whenever possible were collected in a given channel concurrently. The spatial distribution of ADCP and GPS data can be seen in Figure 3-1, and collected ADCP data is shown in Table 3-1 The deployment was timed to neap tides so that downstream water level fluctuations did not significantly influence our results (Figure 3-4). Baptiste Collette was surveyed on March 31st, and then a repeat survey was performed on April 3rd. The passes of The Jump and Cubit's Gap were surveyed on April 1st and 2nd, respectively. The highest water surface elevation range (6 cm) occurred during the first day of the deployment, March 31st.

Path	Inlet Q_w (m^3/s)	Outlet Q_w (m^3/s)	Discharge Fraction Lost	Mean Inlet Velocity (m/s)	Mean Outlet Velocity (m/s)	Inlet Area (m^2)	Outlet Area (m^2)	Water Surface slope	Bed Slope
BC1 Day 1	1643	1115	0.32	1.43	1.68	1146	665	-6.03×10^{-5}	3.70×10^{-4}
BC1 Day 4	1862	1239	0.33	1.61	1.69	1157	733	-6.03×10^{-5}	3.70×10^{-4}
BC3 Day 1	524	93	0.82	1.07	0.92	488	100	-7.29×10^{-5}	5.20×10^{-4}
BC3 Day 4	563	109	0.81	1.14	0.99	494	110	-7.29×10^{-5}	5.20×10^{-4}
CG1	2021	901	0.55	1.29	0.93	1570	966	-3.49×10^{-5}	6.90×10^{-5}
CG2	1078	85	0.92	1.14	0.72	922	118	-4.66×10^{-5}	1.80×10^{-4}
GT1	813	141	0.83	0.53	0.57	1508	245	-4.73×10^{-5}	6.10×10^{-4}
GT2	1033	177	0.83	0.97	0.40	1070	438	-4.34×10^{-5}	6.50×10^{-4}

Table 3-1. Summary data from each channel.

All columns are derived from ADCP data except Water Surface Slope, which is derived from GPS data, and Bed Slope, which we calculate using both ADCP and GPS data. Inlet area and discharge are summed across the north and south forks of CG2, and the velocity is averaged.

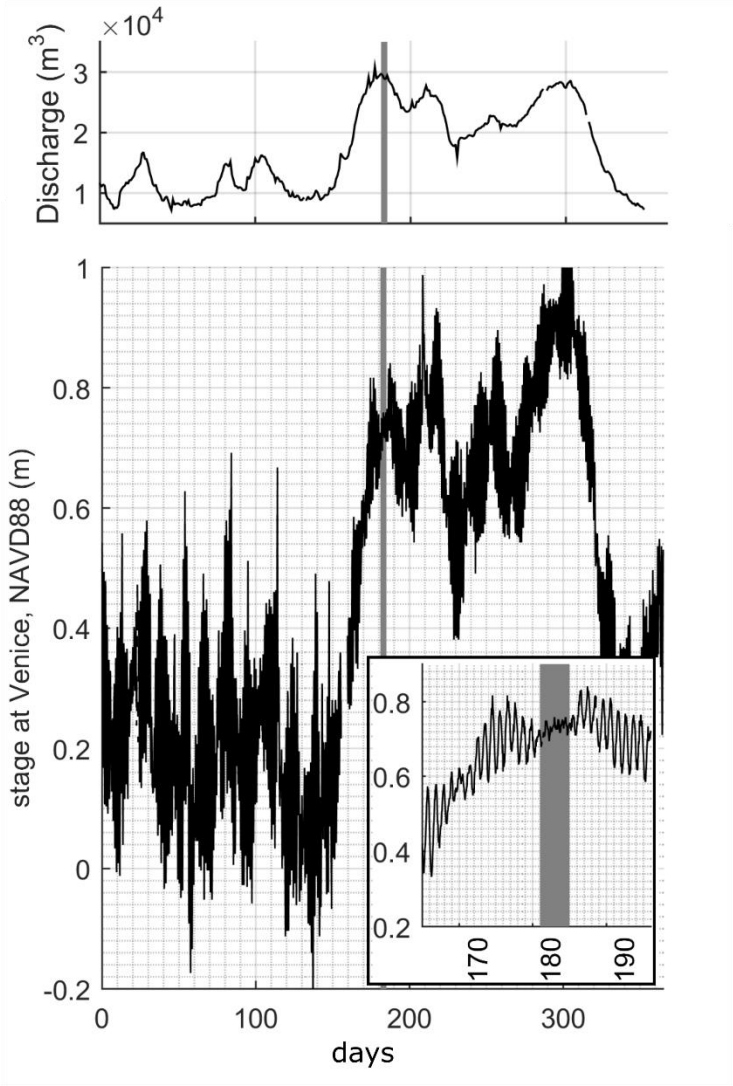

Figure 3-4. River Stage.

River Stage at the Venice Gage, located in the Mississippi River trunk channel at River Kilometer 17, on the West Bank, just north of the entrance to Grand Pass. The x-axis is shown in days since the beginning of the 2015 water year, on October 1, 2014. Field deployment days are highlighted in gray in the main image and in the inset. The amplitude of the tidal signal during the deployment was approximately 2 – 6 cm, compared to 20 – 30 cm which is typical at spring tides. Trunk channel discharge measured at Belle Chasse is shown in the top frame.

3.4.1 Water Surface Elevation

We surveyed water surface elevation along the bank of each channel with a Trimble R8 GNSS Survey System, using RTK correctors from GulfNet at LSU's Center for Geoinformatics. When collecting measurements the GPS was mounted on a 2 m pole and used to determine the bed elevation near the channel banks, which were only accessible by boat. We then measured the water depth on the pole and combined the two numbers to get water surface elevation. Where the bank was not accessible by boat we used pilings to stabilize the GPS. Measurements were collected when the GPS was stable for 3 seconds. When the GPS could not be held stable we used the average of three instantaneous measurements. Measurements in Baptiste Collette and The Jump were collected approximately 500 m apart, while measurements in Cubit's Gap were collected at 1000 m intervals. The water surface slope in each channel was estimated with a linear fit to the data.

3.4.2 Flow Parameters

We collected flow parameters and hydraulic geometry with a Teledyne RDI 600 kHz RiverRay Acoustic Doppler Current Profiler (ADCP) mounted towards the stern of the R/V Mudlump to collect channel velocity cross sections, discharge, and geometry data. ADCP transects were collected at approximately 3000 m intervals along channel, and downstream of every major bifurcation. Within each cross section, horizontal resolution was approximately 1-2 m, depending on the boat speed. Vertical resolution varied by water depth, but ranged from 20 cm in the shallowest channels to 80 cm in the

deepest. Cross sectional data were post processed using WinRiver II to calculate discharge, velocity, and channel cross sectional area. Mean velocity was calculated by dividing the measured discharge by the measured cross sectional area at each transect. Velocity percentiles were calculated by resampling the measured velocities onto a regular grid (0.5m horizontal by 0.2 m vertical). We calculated Froude Number using mean velocity and median transect depth. The ADCP profiles were also used to provide channel bathymetry transects. Each ADCP transect profile was latched to our estimated linear water surface elevation profile in order to calculate the channel bed elevations shown in (Figure 3-2). We use the method of Engelund and Hansen (1967) to estimate rates of sediment discharge per unit channel width. (see eq. 5, in Modeling section)

The USGS standard procedure when collecting discharge measurements with an ADCP (Mueller et al., 2009) is to survey a transect a minimum of four times. We were limited in time, and only collected a single transect at each sampling location. Where repeat measurements were taken our data suggest an error of ±10%. Because our analysis is more dependent on the downstream trend of discharge than on the absolute magnitude at any location we chose to accept a reduced accuracy in our discharge measurements in exchange for broad geographic coverage.

3.5 Field Results

3.5.1 Trends in Flow Properties and Channel Geometry

We display the long profile of channel hydraulic properties for the channels of each network in Figure 3-2. Water surface slope ranges from 3.49×10^{-5} in Cubit's Gap (CG1) to 7.29×10^{-5} in Baptiste Collette (BC3), with channel slopes in The Jump similar to those observed in Cubit's Gap. The differences in slope are consistent with the distance from the river to the shoreline, which is shortest in Baptiste Collette, at 12 km, compared to 17 km in Cubit's Gap and Grand Pass; and with lower water surface elevation in the river at Cubit's Gap. Though a slight curvature is visible in some channels, the linear fit yielded an R-square value of at least 0.90 in all channels and no other elementary function seemed appropriate. Data collected during the repeat survey of Baptiste Collette shows that water surface elevations at a given location differed by a maximum of 8 cm, and usually less than 3 cm, without any consistent trend. ADCP derived properties were also similar during both surveys. For our analysis we group the survey data from both days in Baptiste Collette together. (Table 3-1)

Channel bed slopes measured from the thalweg depths are usually adverse, with slopes an order of magnitude greater than the water surface gradient. As with water surface gradient, the channels of each network share similar bed gradients. The decrease in cross sectional area that is evident with downstream distance in all channels is driven by channel shallowing, not by the water surface gradient. Width to depth ratios, which range from ~10 to ~30, are similar within each network (Figure 3-2). The exception to this trend is Cubit's Gap Main Pass, which is extremely wide relative to its depth. In all

channels, cross sectional area decreases downstream as the channels get shallower and narrower.

Velocities are highest in Baptiste Collette, with mean velocity clustering near 1 m/s in BC2 and BC3, and 1.5 m/s in BC1. The Jump features the lowest mean velocity, hovering near 0.5 m/s throughout GT1, and near 1 m/s in GT2. 95^{th} percentile velocities are 0.2 to 0.5 m/s faster than mean velocities, with greater differences observed in the larger channels. All channels maintain their velocity throughout most of their length, slowing down only in the final kilometers.

3.5.2 Along-Channel Flow Loss

A critical feature of the distributaries in our study site is that nearly all of them lose flow along their length (Figure 3-2, Table 3-1). The only exception is BC2, in which the discharge increases by ~10% from overflow of the adjacent channels BC1 and BC3. For this reason, BC2 is excluded from further analysis. The largest channels in Baptiste Collette and Cubit's Gap, BC1 and CG1 respectively, each lose 55% of their flow before the outlet, while the smaller channels (BC3 and CG2) lose 80% and 90%. In The Jump, where the channels are more nearly symmetric at their bifurcation, GT1 loses 91% of its input and GT2 loses 83%. The smaller channels, as measured by cross sectional area, tend to lose more flow than the large ones.

3.6 Model of Gradually Varied Flow with Flow Losses

To set our expectations regarding the influence of channel geometry and flow loss in the backwater reach we use a 1D model of gradually varied flow. The model simulates instantaneous conditions in a channel, but does not address the interaction of channels in a network or their evolution. We use a hydraulic model described by Cui and Parker (2005), which is derived from the St. Venant equations, plus an additional friction term to account for the lateral flow losses [*personal communication, Chenge An]*.

3.6.1 Model Description

We begin with a Saint Venant Equation and include a flow loss term, but remove all time derivatives under the assumption of steady flow:

$$\frac{\partial}{\partial x}\left(\frac{Q_w^2}{A^2}\right) = -g\frac{\partial H}{\partial x} + g\left(S_0 - S_f\right) \tag{2}$$

$$\frac{\partial Q_w}{\partial x} = q_{wl} \tag{3}$$

where x is the streamwise coordinate, Q_w is the in-channel water discharge, $H(x)$ is the local flow depth, $g = 9.8\frac{m}{s^2}$ is the acceleration due to gravity, q_{wl} is the width-averaged lateral flow input, and A , the channel cross sectional area, is the product of channel width, $B(x)$, and $H(x)$. S_0 is the bed slope, $S_f = n^2\frac{u^2}{R^{4/3}}$ is the friction slope, u is the mean channel velocity, R is the hydraulic radius, and n is Manning's n. Applying the quotient rule to equation (2) then substituting equation (3) into the result and dividing by g yields:

$$\frac{2Q_w q_l}{gA^2} - \frac{2Q_w^2}{gA^3}\left(B\frac{\partial H}{\partial x} + H\frac{\partial B}{\partial x}\right) = -\frac{\partial H}{\partial x} + S_0 - S_f \quad . \tag{4}$$

We introduce the Froude number in the form $F = \frac{Q_w}{A\sqrt{gH}} = \frac{Q_w\sqrt{B}}{\sqrt{gA^3}}$, and define $S_l = \frac{2Q_w q_{wl}}{gA^2}$ as an additional friction term that accounts for lateral momentum exchanges. Substituting and rearranging terms gives us the final form of the backwater equation that we will use:

$$\left(1 - F^2\right)\frac{\partial H}{\partial x} = F^2\frac{H}{B}\frac{\partial B}{\partial x} + S_0 - S_f - S_l \tag{5}$$

We apply equation (5) to a rectangular channel whose width does not change along stream, so in practice the $\frac{\partial B}{\partial x}$ term is zero within the channel. Equation (5) is solved by numerical integration beginning at the downstream end. The procedure is described in detail below.

The channels we observe in the field lose flow through shallow (<1 m) cuts in the levees and by overbank flow. In this case most flow exits the channel perpendicular to its downstream axis, and momentum is lost only as a consequence of fluid mass loss. We use the S_l term in our model to reflect this behavior. The streamwise plots of water discharge in the field (Figure 3-2) show an approximately linear decrease in discharge in all channels. In keeping with these data we impose flow loss along our channel (via q_{wl}) such that the volume of flow lost per unit distance is constant along the channel.

Following Lamb et al. (2012) we use a spreading plume beginning at the shoreline to make the modeled water surface elevations in the channel match our field observations more closely, and to lessen the discontinuity in water surface elevation at the shoreline.

The plume is applied by setting the width offshore to $B = B_{channel} + 2(x - x_{sl})\tan(\theta)$, where $B_{channel}$ is the channel width at the shoreline, $(x - x_{sl})$ is the distance from the shoreline, and θ is the plume spreading angle. No flow is lost in the plume portion of the domain, which is imposed by setting S_l to zero in the offshore cells. The purpose of the plume is to allow the flow depth at the channel mouth to arise as a model outcome rather than an imposed boundary condition. Lamb et al. (2012) found that the results in the channel were insensitive to plume spreading angles greater than 1^{o}, and that plumes in nature range from 5^{o} to 13^{o}. We choose a spreading angle at the upper end of this range, 13º, in order to allow significant spreading over our flat offshore bathymetry.

We run our model over bathymetry that is patterned after the Baptiste Collette channels, which come closest to our ideal of having a large and a small channel both of which lose flow through levee cuts and overbanking. The channel portion of the domain is 8 km long, and has an adverse slope of 2.5×10^{-4}. The plume portion of the domain continues offshore for 2 km, with zero slope. A flat offshore region for 2 km is consistent with the modern bathymetry offshore of Baptiste Collette and Cubit's Gap (NOAA, 2011a, 2011b).

3.6.2 Model Implementation

To initialize a model run we first define the bed elevation, channel width, and local water discharge at all nodes. We then apply a water surface elevation at the downstream end of the plume and solve sequentially upstream with a first-order finite difference scheme. We perform this calculation for Manning's n values ranging from 0.01 to 0.03, in increments of 0.001, which is appropriate for large sand bedded rivers

(Arcement and Schneider, 1989). For each value of Manning's n we adjust the tailwater elevation until we obtain a solution that 1) has a water surface elevation of zero at the shoreline, and 2) has a 60 cm water surface elevation difference between the channel entrance and the shoreline. Adjusting Manning's n affects S_f in a way that is functionally equivalent to the dimensionless friction parameter used by Nittrouer et al. (2012b), but can also be used in our sediment transport model. Model runs that cannot meet these conditions within a 1 cm tolerance are thrown out as having unreasonable combinations of discharge and channel geometry. We choose 60 cm because this is the approximate water surface elevation decrease along the Baptiste Collette channel.

Sediment transport rates are calculated at every node in the domain using the method of Engelund and Hansen (1967) to calculate total sediment load:

$$q_s = \frac{0.1}{f}\left(\frac{HS_f}{(s-1)d}\right)^{\frac{5}{2}}\sqrt{(s-1)gd^3} \tag{6}$$

where s is the specific gravity of quartz relative to water, and d is the mean grain diameter, which we take to be 150 μm. The nondimensional friction factor f is defined by $f = \frac{2S_f}{Fr}$. We calculate the spatial divergence of the sediment transport field, $\frac{\partial q_s}{\partial x}$, to indicate which parts of the domain are most likely to be sediment sources or sediment sinks. Ignoring sediment supply or bed material considerations, a reach with a positive divergence is prone to bed scour, and a reach with negative divergence is prone to deposition.

3.7 Model Results

We apply our model to idealized distributary channels that are patterned on our field sites. The focus of the analysis here is on channels that are similar to those found in Baptiste Collette, BC1 and BC3. We choose these channels over those of Cubit's Gap and The Jump because of their simple planform and their lack of large bifurcations or confluences. Each channel we model is 8 km long, approximately the distance from the last major bifurcation to the shoreline of the channels in Baptiste Collette. They share the same adverse bed slope of 2.5×10^{-4}. The channel dimensions are tuned so that the velocity at the shoreline is approximately that observed in the field, and the along channel velocity trend matches the field observations. Detailed model inputs are given in Table 3-2. Once a model is validated for field conditions we perturb it by altering the along channel flow loss in increments of 10%.

Model outputs can be seen in Figure 3-5. The blue line in each plot is the modeled condition whose flow loss is most similar to our field observations, and while these are not direct simulations of field conditions, the comparison is intended as a model validation. For example, Channel BC1, the larger of the channels we study in Baptiste Collette, lost approximately 30% of its input discharge before reaching the shoreline. Despite the 30% flow loss, velocity increases steadily along the channel as it does in our field observations (Figure 3-2). The increase in mean velocity drives an increase in sediment transport capacity, which in turn would be predicted to cause bed scour near the channel mouth. By contrast the small channel, which is of the approximate dimensions of BC3 and loses 80% of its flow, keeps nearly constant velocity and sediment transport along its entire length.

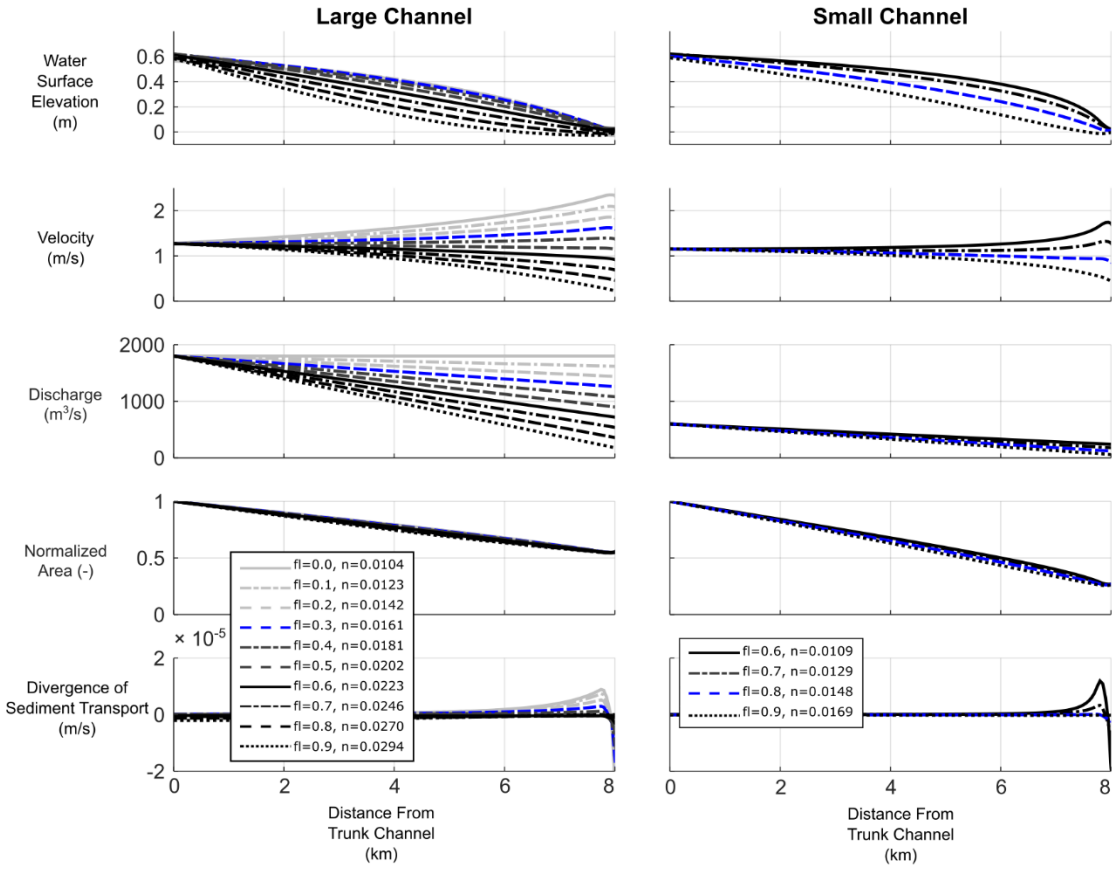

Figure 3-5. Model Results.

The blue line represents the model run that is closest in flow loss to the field conditions observed in BC1 (Large Channel) and BC3 (Small Channel). Legend values show the fraction of flow lost (fl), and the modeled Manning's n.

	Large Channel	Small Channel
Channel Length (m)	8000	8000
Channel Bed Slope (-)	-0.00025	-0.00025
Plume Length (m)	2000	2000
Plume Bed Slope (-)	0.001	0.001
Q_{w_in} (m^3/s)	1800	600
Width (m)	250	150

Table 3-2. Parameters used to initiate the models shown in Figure 3-5.

The effects of perturbing the channel from this condition are not symmetric. Reducing the flow loss from 0.3 to 0.1 in the large channel results in an increase in velocity at all points in the domain, and increased divergence in the sediment transport field towards the shoreline, indicating potential bed scour. However increasing the flow loss along the channel from 0.3 to 0.5 does not significantly alter the divergence of the sediment transport field, and therefore no substantial bed adjustment would take place as a result of the change..

The 80% loss observed in BC3 is sufficient in our model to maintain the channel in its current state as a sediment conduit that neither erodes nor deposits. Reducing that flow loss to 0.7 or 0.6 would cause a significant increase in velocity near the shoreline, driving a large increase in potential scour near the channel mouth. Further increases in channel flow loss lead to untenable friction coefficients, so those model runs were removed from consideration. A flow loss of 80% is very near the limit of our model. Increasing flow loss to 90% results in only slightly more deposition near the channel mouth.

It is notable that the channels of a given distributary network share similar bed slopes. Because the two branches of a given bifurcation share common water surface elevations upstream as well as downstream, both channels must experience the same head loss, which for channels of equal slope implies an equivalent loss of flow depth. Because the small channel is shallower than the large one, a given decrease in flow depth causes a proportionally larger decrease in cross sectional area, and thus a larger increase in mean velocity. In this particular case the combined result is that the shallower channel’s cross sectional area decreases by over 75% along the length of the channel while the large

channel's area decreases only by 45%. For this reason the small channels in our model are much more sensitive to variations in flow loss than the large ones. In the field the smaller channels respond by losing proportionately more flow than the large ones. We also note that the water surface slopes are an order of magnitude less than the bed slopes, and that water surface elevation varies only by decimeters between model runs at any location. The trends in cross sectional area that drive velocity and sediment transport are driven by bed geometry, as is the case in the trunk channel (Nittrouer et al., 2012b).

3.8 Discussion

3.8.1 Distributary channel network stability and the q_s* stability metric

We presented data collected during flood conditions in the primary distributary channels of three subdelta distributary networks. All of the channels from which we collected data experienced significant flow loss along their length. In two of the three channel networks (CG, BC) the channel that took less flow at the inlet lost a greater percentage of that flow along its length. In the third channel network (GT) both channels lost 83% of their inlet flow, which is similar to the losses experienced by the smaller channels in the other two networks. Our field data is collected during a single flood, and long-term data documenting the evolution of flow distribution within the channel networks does not exist. But we do know from serial mapping in Baptiste Collette and Cubit's Gap (Figure 3-3) that the locations and relative widths of the primary subdelta distributaries have stayed constant throughout ~100 to 150 years of activity in these two channel networks. We therefore surmise that the division of flow and sediment between

the primary distributaries in each network has not changed systematically over its lifespan. This fulfills the criterion for bifurcation stability that was suggested by Kleinhans et al. (2013). With that in mind, our data set suggests that flow loss could play an important role in maintaining distributary channel networks that has not yet been examined.

We are unaware of any studies of bifurcation dynamics that have considered flow loss along the bifurcates. But our observation that significant differences in flow loss can persist among the channels of a stable network suggests that flow loss is an important parameter. Our data set presents an opportunity to examine flow loss as an unrecognized mechanism that can maintain deltaic distributary networks in stable configurations. As an indicator of channel stability we introduce q_s^*, which is the ratio of sediment transport capacity per unit width at the channel outlet to that at the input. Channels with high q_s^* values are expected to undergo net erosion over their length. Conversely, q_s^* less than one indicates an infilling channel, and q_s^* values near 1 indicate a stable channel that is able to transport the sediment that it receives upstream through its entire length. In a stable bifurcation we would expect q_s^* to be nearly equal to 1 in both channels.

We use our model results (Figure 3-5) to display q_s^* as a function of flow loss (Figure 3-6). Field results from Baptiste Collette plot in line with the modeled trend and plot near q_s^*=1, implying that the field case represents a stable channel configuration. We also observe that the slope of the flow loss vs q_s^* plot is steeper for the small channel in the vicinity of q_s^*=1, implying that the small channel is more resistant to perturbations than the large one, because a small decrease in flow loss is met with a large increase in erosion. Our results suggest that small changes in flow loss, for example by crevassing or

crevasse healing, can bring channel trends in to agreement in an asymmetric bifurcation. This result is relevant to river management efforts in deltas worldwide, and also raises the possibility that autogenic fluctuations in flow loss can play a role in maintaining a channel network in a stable configuration.

In order to use q_s^* as an indicator of stability we must make the assumption that the upstream end of the channel is approximately in equilibrium with the amount of water and sediment that it receives from the parent channel, but that channel infilling and channel expansion both originate from the channel tip. This is different from some bifurcation models (e.g. Bolla Pittaluga et al., 2015) that model siltation as initiating upstream near the bifurcation node, but is consistent with data in dynamic delta environments that show channel change initiating from downstream (Shaw and Mohrig, 2014). The principle drawback of q_s^* is that, analogous to thermodynamics vs. kinetics in physical chemistry, it tells us whether a change in channel configuration is likely to occur, but provides no information about how quickly. Nittrouer et al. (2012b) productively used the divergence of the 1D sediment transport field to examine the net impact that oscillations between low flow and flood conditions have on the channel bed. This is an excellent method of assessing regional trends, and provides information about the speed with which a channel is changing, but does not provide an accessible way of making comparisons between channels. We use the q_s^* here because it explicitly ties the fate of a channel to its mouth dynamics, and because it can be used to compare channels with ease.

Along-channel flow loss is a new addition to the literature on distributary channel network stability, which has typically been studied by examining the morphodynamics of

river channels in the immediate vicinity of bifurcations. For example, Kleinhans et al. (2011) showed through a combination of numerical modeling and stratigraphic reconstruction that the position of a bifurcation along a meander can play an important role in the bifurcation's evolution, as the complex flow patterns in the meander tend to favor one branch over the other. This is in line with other studies (Hardy et al., 2011; Miori et al., 2012) that have found that secondary circulation structures associated with channel planform curvature play an even more important role in bifurcation evolution than do moderate water surface gradient advantages. Likewise, high angle bifurcations are often understood as locations of complex flow that causes intense local deposition. In fact, Welder (1959) documented the process of channel closure at several high angle bifurcations to secondary and tertiary channels in Cubit's gap in 1953. He observed, over the course of a single flood season, bars growing across the mouths of several channels. These bars resulted in recirculation eddies that directed sediments to settle in the inlet throat. It is interesting to note though, that some of the channel throats that Welder observed clogging more than a half century ago remain navigable today.

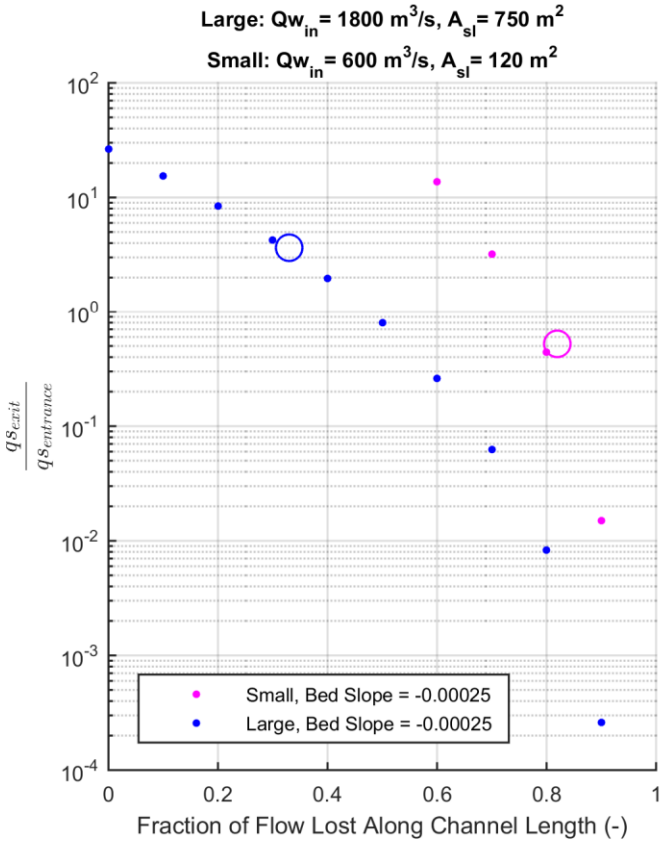

Figure 3-6. Fraction of Flow Lost vs. q_s^*

Ratio of width averaged sediment transport rate at the exit to the entrance of two modeled channels. The large and small modeled channel geometries are similar to BC1 and BC3, respectively. Field results from BC1 and BC3 are plotted as open circles in the parameter space.

3.8.2 How much flow do unmanaged channels lose?

Analyses of overbank environments in modern (Lewin et al., 2016) and prehistoric (Shen et al., 2015) rivers point to flow loss as integral to the function of the channel, but there are very few data sets that can be used to quantify flow loss throughout a significant reach of a large river prior to major anthropogenic modification. However, the 1867 report of Humphreys and Abbot to the United States Bureau of Topographical Engineers does contain a comprehensive analysis of flow lost to crevasses from Helena, Arkansas to New Orleans, Louisiana during the flood of 1858 on the Mississippi River. Discharge in the river was obtained by measuring cross sectional area with lead lines, and measuring velocity at various depths with weighted floats. Discharge to the crevasses was considerably more difficult to obtain, but the measurement principles were similar to those in the river. The largest source of error in measuring the crevasse discharge was in extrapolating between measurements in a crevasse whose dimensions were rapidly changing. At the peak of the flood, the discharge passing Vicksburg, MS was approximately 35,000 m^3/s, which nearly coincides with the 33,000 m^3/s that is required to elevate the river at Vicksburg above the surrounding landscape today. In the modern river this value is exceeded almost annually (Ramirez et al., in review) In 1858, this discharge was sufficient to cause widespread levee failure and inundation beyond any other flood observed since 1798 (Humphreys and Abbot, 1867) . Of the discharge that passed Vicksburg in 1858, 17% was lost to crevassing between Vicksburg and New Orleans, not including losses to the Atchafalaya River (Figure 3-9). The river was confined by levees at this time, so all of the crevasses tabulated were the result of levee failures that evolved rapidly throughout the course of the flood, rather than natural

crevasses with relatively stable configurations. We consider this data to represent a lower bound on the amount of flow lost to crevassing from the main channel of the Mississippi River prior to anthropogenic modification.

In the Wax Lake Delta, which is a subdelta at the coast, and of similar scale to the subdeltas we study in the birdsfoot, two recent studies have found significant flow loss throughout the distributary network. Shaw et al. (2016) infer patterns of flow offshore of the Wax Lake Delta, and are able to deduce that during a large flood event 59% of the combined discharge of two adjacent distributaries exits the channels before arriving at the subaqueous channel tips. This estimate includes flow that is lost over the subaerial levee as well as the subaqueous levee beyond the shoreline, and to cuts in both. Hiatt and Passalacqua (2015), working in the same Wax Lake Delta channels, but during low flow conditions, study the flow lost in two passes between their shared upstream difluence and the shoreline. Their data show that when the tides are not considered, one pass loses approximately a quarter of its flow and the other loses approximately half. The losses experienced in the Wax Lake Delta are of a similar magnitude to those of the subdeltas in the birdsfoot delta.

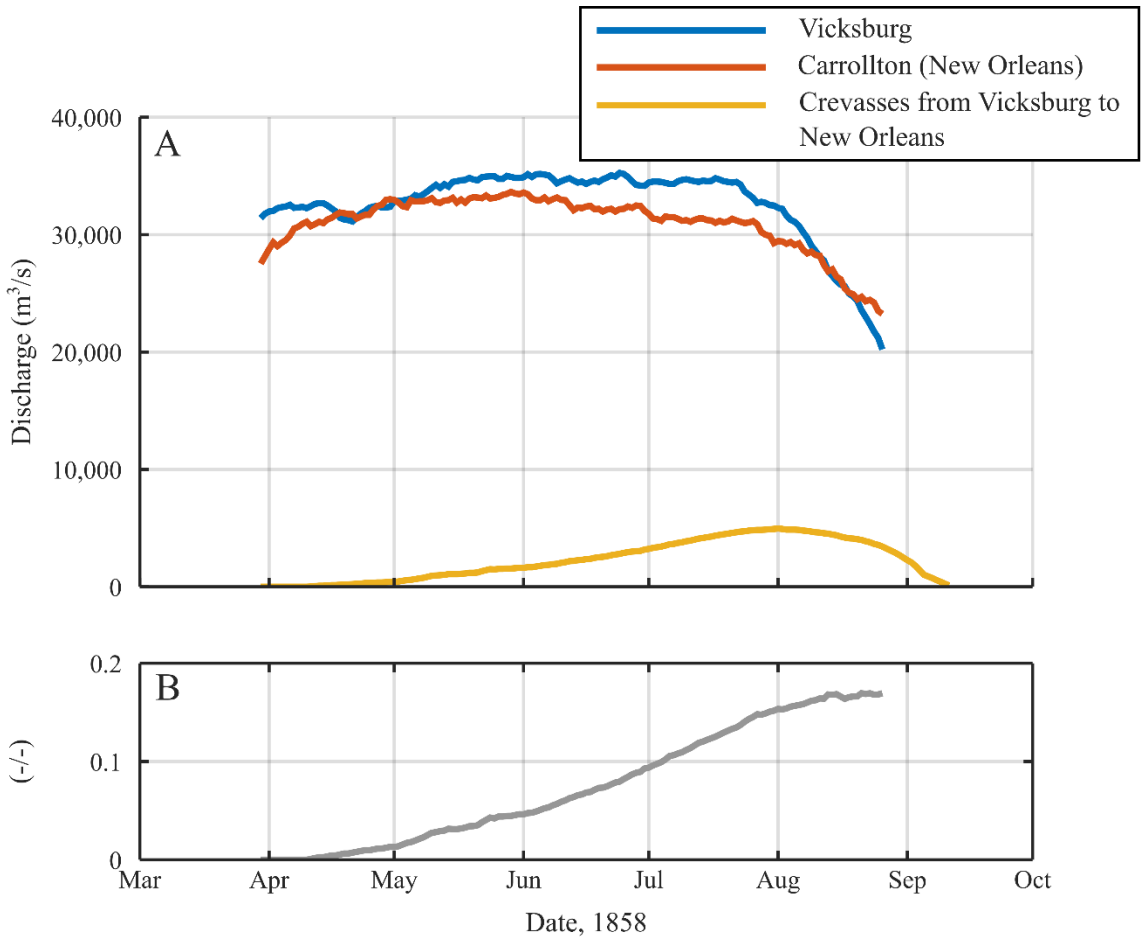

Figure 3-7. The Flood of 1858

A: Mississippi River discharge at Vicksburg and New Orleans during the flood of 1858, and total discharge from crevasses along the reach from Vicksburg to New Orleans. B: Crevasse discharge as a fraction of Vicksburg discharge. Data is from Humphreys and Abbot (1867), and is collected in the SI.

3.8.3 Channel Bed Response to Flow Loss in the Backwater Reach

Our model results and field data taken together demonstrate that when terminal distributary channels are not confined they can satisfy the geometric constraint imposed by base level by adjusting their capacity to convey flow, as well as by the established mechanisms of increasing velocity or scouring a deeper bed. The same equation that we use to model flow in the terminal distributary channels (Equation 5) has been used to model the flow and sedimentary response in the backwater reach of the Mississippi River truck channel (Nittrouer et al., 2012b), albeit without the imposed flow loss term. The flow loss term was not considered by Nittrouer et al. (2012b) because the Lower Mississippi River, with the exceptions of the diversion to the Atchafalaya River and intermittent losses to the Bonnet Carre spillway, is prevented from losing flow by manmade levees above River Kilometer 35 (Allison et al., 2012). Our results, however, show that flow loss can play an important role in modulating flow and sediment transport in distributary channels. In this section we apply the lessons that we learned in the terminal distributaries about flow loss to investigate the extent to which the sediment dynamics of the Lower Mississippi River may have been altered by the modern levee system.

Studies in the modern Lower Mississippi River have shown evidence of bed erosion downstream of New Orleans (RK 161), including channel deepening (Galler et al., 2003), reach-scale removal of bed volume (Little and Biederharn, 2014), hydrodynamic conditions that are conducive to bed scour (Nittrouer et al., 2012b), and exposed substrate (Nittrouer et al., 2011; Viparelli et al., 2015). But it is not clear from

the existing analyses whether erosion towards the coast is a result of the flow confinement, or is inherent to large alluvial rivers in their lower reaches. The model of gradually varied flow with lateral flow loss that we presented above can also be used to consider whether the bed morphology of the Mississippi River could have been altered by the advent of the modern flood protection system. To do so we apply our 1D model to a hypothetical river with dimensions, slope, bed sediment caliber, and discharge similar to those of the Lower Mississippi River. Our model is similar in spirit to that of Nittrouer et al. (2012b), but with a channel that can lose flow along its length. We calculate the divergence of the sediment transport field, which we use to compute the potential bed elevation change over the course of a year, first for the case of full flow confinement, and then for the case of 10% flow loss during flood conditions only, applied evenly along the lower 800 km.

The results, shown in Figure 3-8 and Figure 3-9 suggests that the effects of flow loss are most influential towards the shoreline. When flow is confined in the channel, velocity is maintained all the way to the outlet, causing divergence in the sediment transport field, and a high potential for erosion in the lower reach. But if even 10% of flow is lost throughout the channel, the resulting decrease in velocity near the shoreline results in a sharp reduction in sediment transport capacity, and a sharp increase in potential aggradation. Available data from the Lowermost Mississippi River shows bed degradation in the reach below New Orleans until ~River Kilometer 35 (Galler et al., 2003; Nittrouer et al., 2011; Little and Biedenharn, 2014 as shown in Figure 3-10, herein), and this analysis suggests that that pattern is enhanced by the flow confining levee system currently in place. The response to flow loss is not as strong at the upstream

end of the backwater reach. There the effect of allowing 10% flow loss is a slight increase in potential sedimentation rate relative to the flow confined case, but the difference is not easily distinguishable from the difference between the two cases in the normal flow reach further upstream.

The morphological evolution of the Lower Mississippi River's bed is significantly complicated by a number of anthropogenic and natural factors whose onsets overlap in time: diversion to the Atchafalaya River and Bonnet Carre Spillway (Allison et al., 2013; Fisk, 1952; Roberts et al., 2003); upstream changes to sediment supply by dams and bank stabilization efforts (Kemp et al., 2016; Tweel and Turner, 2012); substantial channel shortening by cutoffs (Biedenharn et al., 2000); and a flow confining levee system (Barry, 1998). As a result, no simple explanation of the current bed morphology is appropriate. But our model results suggest that the lower portions of the backwater reach could be deeper as a result of the levee based flood protection system. Overall, the 10% flow loss case suggests a channel bed that is shallower than the present one throughout the backwater reach, but especially so as the river nears the shoreline.

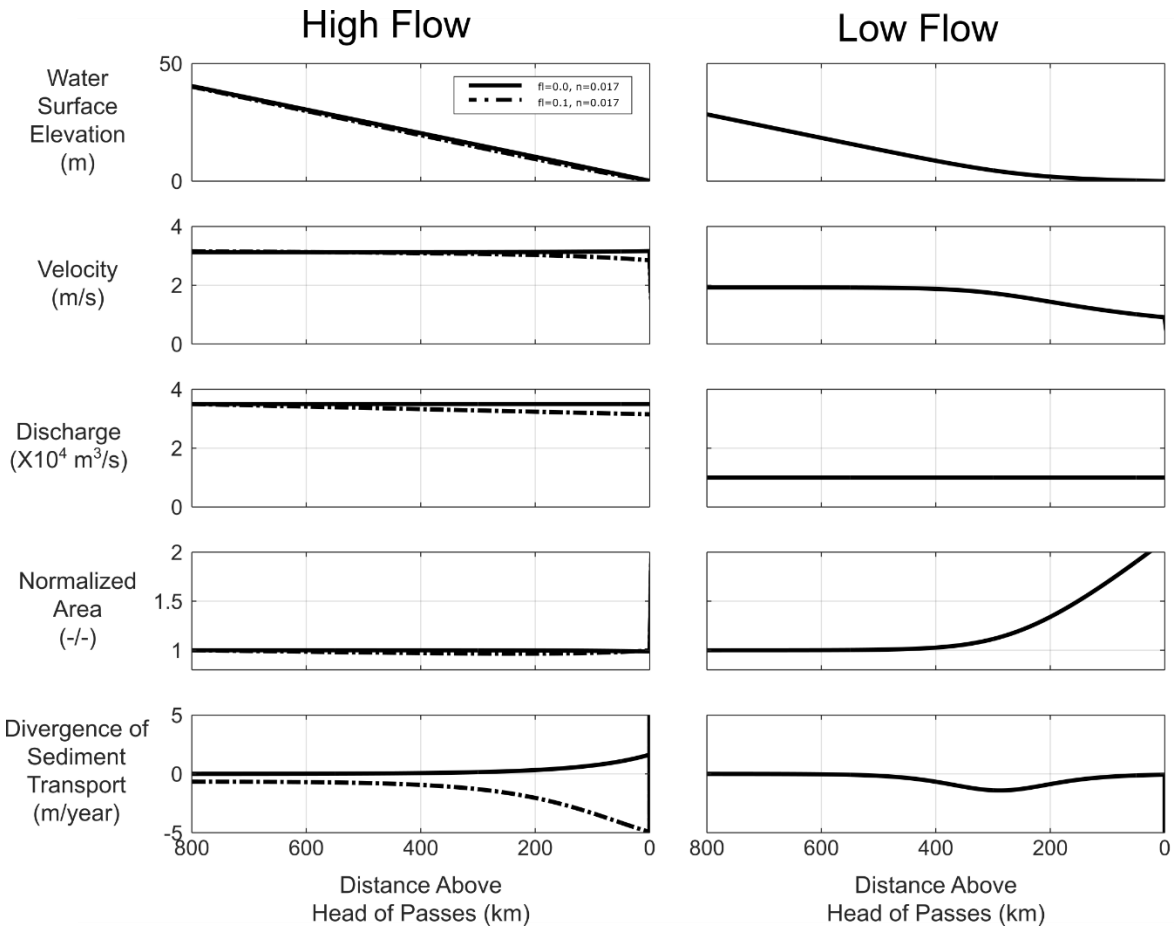

Figure 3-8. Results of 1-D model runs for Mississippi River-like conditions

Results of 1D model runs for Mississippi River-like conditions. Flow loss and Manning's n are shown in the legend. No flow loss was applied during low flow conditions. Note that positive values for the divergence of the sediment transport field correspond to potential erosion, and negative values to potential aggradation. Both cases are of an 800 km river reach with a 20 km spreading plume starting at the shoreline, a rectangular channel that is 500 m wide, and a bed slope of 5×10^{-5}. The flow loss is applied only at high flow. High and low flows are 35,000 m^3/s and 10,000 m^3/s, respectively, and the river is considered to be at high flow for 15% of the time and low flow the remaining 85%. We use a Manning's n of 0.017 for both cases (Arcement and Schneider, 1989).

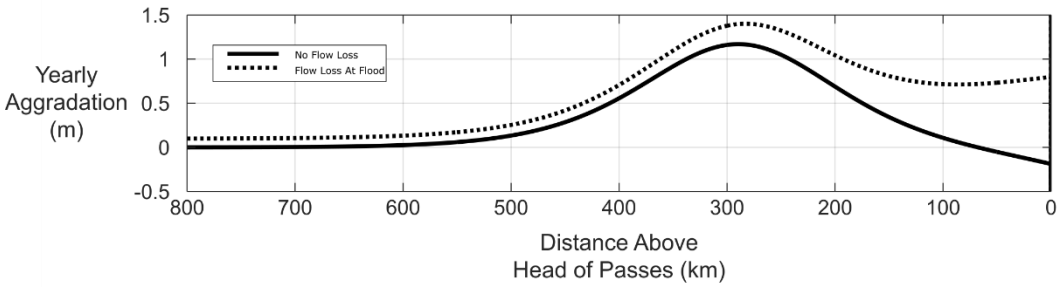

Figure 3-9. Yearly aggradation for the case of 0% flow loss and 10% flow loss.

The difference between the two cases in potential yearly aggradation increases towards the shoreline, suggesting that any impacts from confining flow are likely to be strongest downstream.

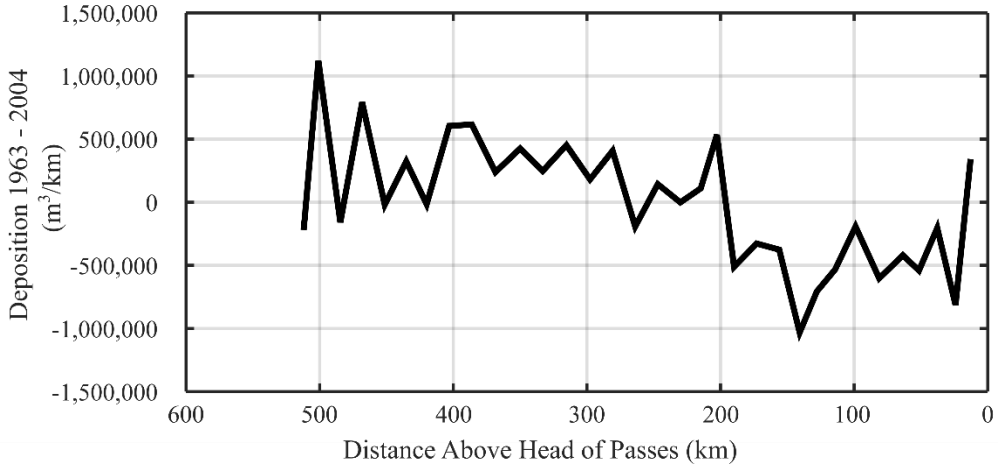

Figure 3-10. Mississippi River Modern Deposition.

Deposition per mile experienced in the Mississippi River from 1963 to 2004. Data used to calculate this figure was extracted from Little and Biedenharn (2014).

3.9 Conclusions

We present hydraulic data collected in the channel networks of three subdeltas to show that flow loss via overbanking and small crevasses is integral to the function of unmanaged distributary channels. Our field observations are supported by a 1D numerical model of gradually varied flow in the backwater reach that is adapted to account for flow loss along a channel's length. We show that velocity and sediment transport trends in the backwater reach are substantially modulated by flow loss; that shallower channels in this reach are more sensitive to flow loss than larger ones are; and flow loss plays an important role in maintaining distributary channel networks in stable configurations. We apply the lessons learned in the subdelta channel networks to the Mississippi River trunk channel, and find that channel bed scour can replace the effects of flow loss in managed channels where loss is prevented. Researchers must take care to account for these effects when applying measurements from modern managed channels to questions of prehistoric morphologic activity.

3.10 APPENDIX

Data tables extracted from Humphreys and Abbott (1867) and Little and Biedenharn (2014) are available in Supplemental Information at http://doi.org/10.5072/FK28054Q27.

4 Sediment Storage Partitioning In Alluvial Stratigraphy: The Influence of Floods

Christopher R Esposito, Diana DiLeonardo, Meg Harlan, Kyle M. Straub

4.1 Abstract

Numerical models of alluvial stratigraphy formation often specify, either explicitly or implicitly, the proportion of channel and overbank sediments that are deposited during a given time. However, little is known about the factors that affect the partitioning of sediment between channels and the overbank environment. Here we use physical experiments to investigate the role that floods play in this partitioning. We find that channels formed under constant flow conditions have low lateral mobility and act mostly as conduits for sediments to reach the shoreline. The bulk of the delta top aggradation in this case is derived from sediment laden flow that escapes the main channels. By contrast, including floods increases channel lateral mobility, and this change is recorded in stratigraphy as an increased proportion of channel relative to overbank deposits. When variable flow is included as an input condition a large volume of in-channel deposition occurs under fluctuating flow conditions, rendering the channels substantial contributors to stratigraphic volume on their own. The increase in channel volume is driven primarily by a threefold increase in the average time that a location on the delta top is subject to in-channel aggradation. Other factors include a slight increase in in-channel aggradation rates, and an increase in erosion in the overbank environment that results from energetic overbank flows. Our study shows that the character of a river's hydrograph exerts a significant influence on the proportion of channel to overbank sediment bodies in alluvial deposits, which is an unexamined source of uncertainty in common stratigraphic models. Our analysis suggests a framework for determining input parameters that are informed by surface processes.

4.2 Introduction

Our eyes and attention are more easily drawn to a river's channel than to the sodden swamps that surround it, but most lowland rivers are embedded in a dynamic overbank environment that plays an important role in managing the channel (Mohrig et al., 2000; Aalto et al., 2003; Hajek and Edmonds, 2014). Mechanisms by which overbank deposition influences channel behavior are well documented. Overbank environment topography and depositional dynamics are known to be important, as avulsion timing and location can be influenced by regional slopes (Slingerland and Smith, 1998), by local features associated with both active and relict channels (Mohrig et al., 2000; Slingerland and Smith, 2004; Jerolmack and Paola, 2007), and by the ability of flow to cause erosion (Hajek and Edmonds, 2014). Bank strength, which is affected by the characteristics of the overbank sediments (Caldwell and Edmonds, 2014) and by vegetation patterns (Tal and Paola, 2007; Nardin and Edmonds, 2014), plays an important role in setting the lateral mobility of channels. And in turn, channel lateral mobility is thought to impact whether a river forms a single thread channel or a branching network (Jerolmack and Mohrig, 2007), implying that the dynamics of the overbank environment play a fundamental role in setting the morphodynamic style of a river, and in the formation of alluvial stratigraphy. Our analysis centers on the fundamental process linking channels and the overbank environment: floods. Specifically, we are interested in the degree to which the character of a river's hydrograph influences the partitioning of sediment between channel and overbank deposits.

The ratio of channel to overbank sediments deposited in a sedimentary basin has long been an important, though implicit, parameter in models of fluvio-deltaic stratigraphy. Some of the earliest models (Allen, 1978; Leeder, 1978; Bridge and Leeder, 1979), function by adding a specified volume of channel and overbank sediments to an alluvial

succession at each time step. The specific volume added of each is determined by the width of the channel belt, the width of the basin, the depth of the channel, the basinwide aggradation rate, and the spatial relationship of aggradation relative to the channel belt, but is consistent for a given model initialization. Post-depositional compaction of fine sediments and erosion by channel belt avulsion events can subsequently alter the ratio of channel to overbank sediment volume that is transferred into stratigraphy. In some cases this alters the topography and dynamically interacts with channel path selection. An important result, consistent through all such models, is that high channel mobility on the surface is associated with high channel body interconnectedness in the deposit. But decreasing the width of the alluvial plain relative to the channel belt – effectively increasing the volume fraction of channel sediment input to the system at each timestep – is also associated with increased channel body interconnectedness. It is therefore important to understand the factors that influence sediment partitioning in order to distinguish between the two similar effects.

The basic framework set forth by the Leeder-Allen-Bridge models – that of a linked channel-floodplain system where channel path selection is driven by floodplain topography, and floodplain deposition is related to channel location – is still in common use in contemporary studies. Törnqvist and Bridge (2002) use field data from the Rhine-Meuse and Mississippi Deltas to fit an exponential decay to overbank deposit thickness as a function of distance from the channel belt edge, and apply this result as an input parameter to a 3D model of alluvial stratigraphy (Mackey and Bridge, 1995). Including realistic topography in this way improves the model, but as with earlier models the channel to overbank deposit proportion input at each timesetep in the Mackey and Bridge (1995)

formulation is determined at the model initialization. This is because, while some variation in the partition of deposit volume is possible due to the geometry of the channel within the computational domain, a given decay constant approximately specifies the channel to overbank deposit ratio. Because the channel to overbank input ratio in Leeder-Allen-Bridge models is heavily dependent on geometric constraints, there is an opportunity to examine in detail the processes that affect the channel to overbank deposit ratio, and thus develop a better mechanism for determining appropriate model input parameters.

While we are unaware of any study that ties the channel/overbank partition to the character of a river's floods, recent years have seen a deluge of interest into whether and how information about flood intensity is transmitted into the stratigraphic record, from the scale of regional channel avulsions (Chatanantavet et al., 2012; Ganti et al., 2014, 2016; Plink-Björklund, 2015) to that of bar dimensions and bedforms (Nicholas et al., 2016; Sambrook Smith et al., 2010; Shaw and Mohrig, 2014; Van de Lageweg et al., 2013). Much of the research into the stratigraphic signature of variable flow has thus far focused on defining sedimentary structures and the geometry of the channel deposits. One point that is often overlooked is that the influence of floods is felt just as keenly in the floodplain as it is in the channel. We present data from two physical basin experiments. One of our experiments features a variable hydrograph and the other was run with constant water and sediment input. We compare the surface dynamics and stratigraphy of the two experiments to test the hypothesis that floods influence channel lateral mobility, and that this plays a role in partitioning sediments between channel and overbank deposits.

Our research is grounded in the field of quantitative stratigraphy, but improving our understanding of sedimentary function in overbank environments is an important goal

across a variety of disciplines. Information about temporal trends in the channel to overbank sediment ratio of a river's deposit can provide important context to stratigraphic reconstructions across climate boundaries (e.g. Foreman et al., 2012), and could factor in to global predictions of fluvial response to climate change (Toonen et al., 2017). Further, the role of overbank environments as sinks for fine grained sediments makes them important to the global carbon cycle (Boye et al., 2017; Sutfin et al., 2016), and our results imply that changes to regional precipitation patterns in response to global climate change (e.g. Scholes et al., 2014) could influence terrestrial carbon budgets.

4.3 Experimental Procedure

We compare results from two physical experiments that differed only in that one was run under constant flow conditions (constant discharge case) (Straub et al., 2015; Li et al., 2016) while the other featured a hydrograph (variable discharge case). Our variable discharge experiment was conducted so that the average sediment and water discharge was the same as in the constant discharge experiment, but that the discharge at flood was three times that at base-flow (Figure 4-1). This discharge ratio is in the range of large rivers in temperate climates like the Mississippi River, but lower than what would be expected in a monsoonal climate (Allison et al., 2013; Plink-Björklund, 2015). Sediment to water ratio was held constant between flood and base-flow conditions. While sediment to water ratio typically varies seasonally in natural systems, we chose to hold it constant in order to clarify the analysis. The sediment mixture used in both experiments is based on the cohesive mixture developed by Hoyal and Sheets (2009), and contains silica flour, quartz sands, bentonite, glass beads, cat litter, and a polymer that increases sediment cohesion. The increase in sediment cohesion adds bank strength that enables single thread channels with sandy beds to form at subcritical Froude numbers. The sediment mixture used here is the "strongly cohesive" mixture used by Straub et al. (2015). Basin dimensions (4.2 m long by 2.8 m wide by 0.65 m deep) and a background sea level rise rate (0.25 mm/hr), which promoted net depositional conditions, were constant between the experiments. (Table 4-1)

The constant flow experiment was paused every 60 minutes to collect topographic and co-registered RGB data of the delta surface with a FARO laser scanner (dry scan). In order to locate flow paths a second scan (wet scan) was taken near the end of each run hour while the experiment was running, with the water dyed blue. Data collection during the

variable flow experiment differed in that RGB data was collected with a digital camera mounted above the basin, and that RGB data was collected once at the end of the run cycle (dry photo), once during the flood (flood photo), and once during low flow conditions (low flow photo). As with the constant flow experiment, topographic data was collected with the FARO at the end of the run cycle. In both experiments the FARO data was interpolated horizontally to a 5 mm by 5 mm grid. The vertical resolution on the laser scanner is approximately 1 mm. The position of the camera used in the variable flow experiment ensured minimal lens distortion on the delta top, and the photographs were latched to the FARO coordinate system with a nonreflective similarity transform and resampled. The image transform was assessed visually to match the scan data within the 5 mm pixel resolution. Each cycle of low and high water conditions in the variable flow experiment lasted 66 minutes, with 7 minutes at flood and 59 minutes at base-flow Figure 4-1. The timing of the flood within each cycle was set so that the delta would be in flood for approximately 10% of each cycle. The length of the cycle is set so that there would be a large number of cycles in the time necessary to aggrade, on average, a single channel depth everywhere on the delta-top, which has been shown to be an important timescale of autogenic activity. The total experimental run time was long enough to aggrade several channel depths, which allows us to assume that the time series behavior of the system parameters that we measure is stationary (Straub et al., 2009; Wang et al., 2011).

We used RGB images, topographic data, and visual assessments to classify each pixel as one of four depositional environments: ocean, channel, overbank, or dry land (Figure 4-2). First we made wet/dry maps by applying a threshold to the ratio $\frac{(blue - red)}{(blue + red)}$ at each pixel for each image. The technique is similar to the NDVI measurement (Tucker,

1979) used to identify vegetation in remote sensing applications, and minimizes the effects of uneven lighting across the delta, and of inconsistent lighting between images.

Because we had both high and low flow images from the variable discharge experiment we were able to set an aggressive threshold that confidently identified deep water in the low flow image, and a less stringent threshold to distinguish land from any water in the flood images. Any pixel that was wet during both high and low flow conditions was considered to be a channel, while pixels that were only wet at high flow were marked as overbank, and pixels that were not wet at all during the cycle were marked as land. We defined ocean as pixels that were wet during all three images, or which had an elevation below the current imposed sea level. The redundant method of defining the ocean results in a shoreline that is always the most conservative. Any pixel that did not fall into one of these defined categories (for example, a pixel that was wet at low flow but not at high flow) was discarded as erroneous.

In the constant flow experiment, where we had a single wet image from each cycle, thus we were not able to use an aggressive color ratio threshold. In practice this meant that the overbank environment could be distinguished from land with a threshold as above, but channels had to be picked by hand. See Figure 4-2 for an example of a picked channel map, and the source photograph. Once the channel maps were defined, the process of defining depositional environments was identical to the variable flow experiment. Slight variations in the basin water surface elevation between high and low flow conditions in the variable flow experiment caused errors in interpreting the depositional environment near the shoreline. To avoid this problem we restricted our analysis, including all figures, and all

calculations, to pixels that were terrestrial (i.e. non-ocean) more than 50% of the time for both experiments.

		Constant Discharge	Variable Discharge, low	Variable Discharge, high
Input Conditions	Q_s (kg/s)	3.91×10^{-4}	3.23×10^{-4}	9.68×10^{-4}
	Q_w (m^3/s)	1.72×10^{-4}	1.42×10^{-4}	4.25×10^{-4}
	sea level rise rate (mm/hr)	0.25	0.25	0.25
	cycle time (min)	60	59	7
	Total run time (hr)	900	186	
Calculated Parameters	maximum channel depth (mm)	15-20	10-12	
	Terrestrial Growth Rate (mm^3/hr)	2.40×10^5	4.70×10^5	
	Average Delta Top Area (m^2)	0.9	1.6	
	T_5 (hr)	64	19	

Table 4-1. Delta Parameters

Forcing conditions and measured morphological parameters for the constant and variable discharge experiments. Sediment and water inputs in the variable discharge experiment are set such that the high discharge is three times the low discharge, and their time integral is equal to that of the constant discharge experiment.

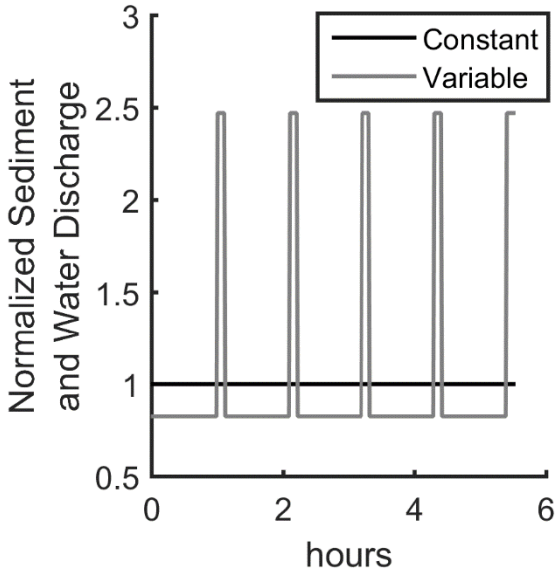

Figure 4-1. Experimental Sediment and Water Discharge

Sediment and water discharge for the constant flow experiment does not vary. Sediment and water discharge during the high flow periods in the variable flow experiment are three times that of the low flow periods, while their time integral is equal to that of the constant flow experiment. Values shown here are normalized by the values from the constant flow experiment.

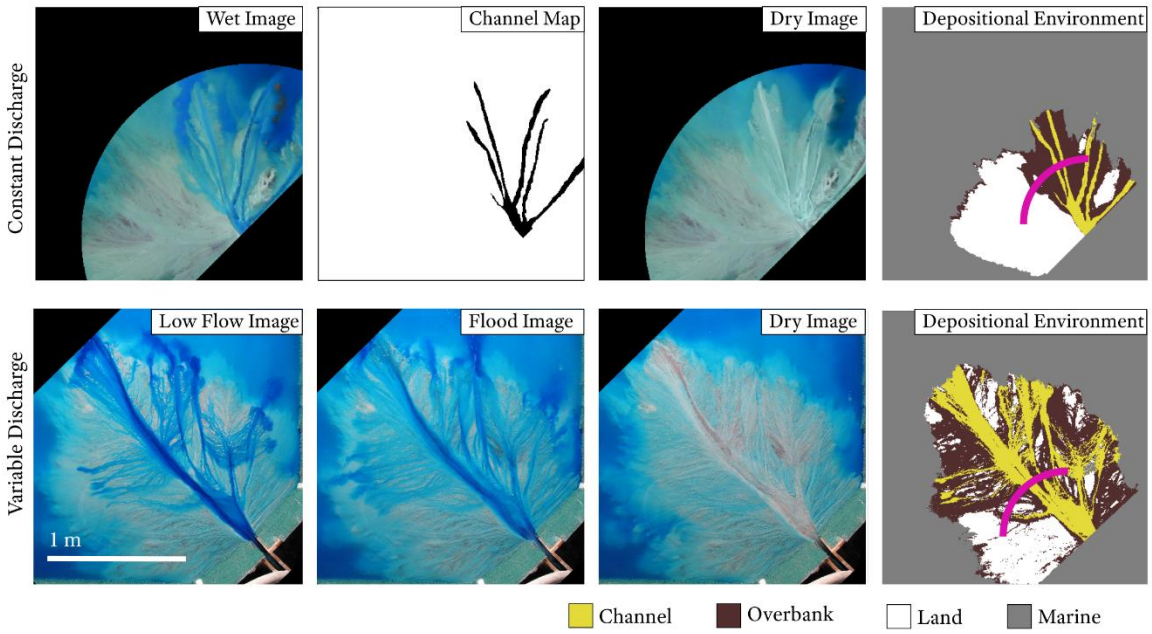

Figure 4-2. Depositional Environments

Maps of depositional environments were generated for each delta using the RGB data, the handpicked channel maps (Constant flow only) and topographic data collected with the FARO laser scanner, of which examples are displayed here. The locations of cross sections shown in Figure 4-7 are marked by magenta lines. Note the small linear features present in the variable discharge overbank environment but absent in the constant discharge case. The constant discharge data shown here is from the cycle ending at hour 452, and the variable discharge data is from the cycle ending at hour 535.4.

4.4 Results

We use our depositional environment maps coupled with our time series of topography to focus our analysis on the role that variable flow plays in channel mobility, and in the partitioning of sediment between channel deposits and overbank deposits. Our first task then is to quantify the deposit volume that is stored in each depositional environment during the experiment. By assigning the aggradation during a timestep in a pixel to the appropriate depositional environment and removing eroded volume, we generated synthetic stratigraphy for the entire delta deposit. We then calculated the fraction of the thickness of each deltaic deposit that is attributable to channel or to overbank deposits. This calculation (Figure 4-3, Table 4-2) shows that 76% of the constant flow stratigraphy is composed of overbank deposits, and only 11% is channel deposit. The remaining 13% is marine deposition or deposition in pixels characterized as land, which occurs occasionally by flows that were not active at the time that the overhead photograph was taken. By contrast, in the variable flow delta the overbank and channel deposit fractions are closer together at 39% and 43%, respectively. The maps of depositional environment and aggradation at each timestep will form the basis for the remainder of our analysis. With the long term average sediment partition established, we use the maps to investigate the transition from short term sediment partitioning to long term, as a function of channel mobility and rates of vertical change in the channel and overbank environments.

In depositional systems where mobile channels are present, channels that migrate through the overbank environment rework sediments that have been deposited there. Some of the reworked sediment will be removed from the overbank environment entirely, implying that the volume of sediment stored in the floodplain should decrease with increasing measurement interval. To investigate the timescales that are relevant to sediment

partitioning, we calculate the fraction of the sediment input that was stored in channel and overbank deposits as a function of the temporal measurement interval, shown in Figure 4-4. For these calculations the total measured change in delta deposit volume was calculated for each possible time interval and divided by the volume of sediment that was input to the basin over that interval. Conversion from sediment mass input (Table 4-1) to volume input was achieved using a deposit porosity of 0.53 and a sediment density of 2650 kg/m^3. The sediment porosity of this sediment mixture was measured by Straub et al. (2015), where it is referred to as the strongly cohesive mixture.

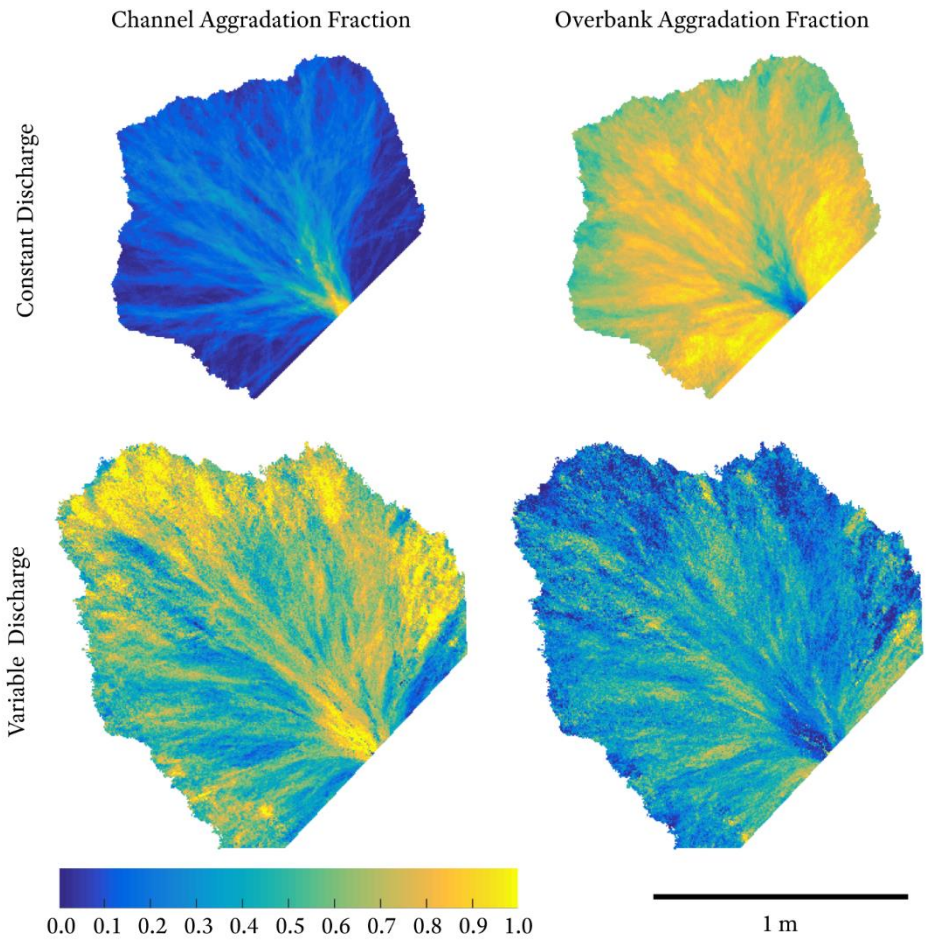

Figure 4-3. Aggradation Fraction

Maps showing the fraction of the total thickness attributable to channelized or overbank deposition. Overbank deposition dominates the constant flow case, but in the variable flow case the observed trend is reversed.

		Channels	Overbank
Variable Discharge	Deposit Volume Fraction (-)	0.43	0.39
	effective aggradation rate (mm/hr)	0.76	0.20
	occupied time fraction (-)	0.22	0.43
Constant Discharge	Deposit Volume Fraction (-)	0.15	0.76
	effective aggradation rate (mm/hr)	0.68	0.43
	occupied time fraction (-)	0.07	0.42

Table 4-2. Aggradation Calculations

Table showing the deposit volume fraction and occupied time fraction for channel and overbank environments. These values are spatial averages of the data shown in Figure 4-3 and Figure 4-5. Effective aggradation rate is derived from deposit volume fraction and occupied time fraction. Note that deposit fractions do not sum to unity. The remainder in each deposit is composed of ocean deposition or deposition in pixels classified as land.

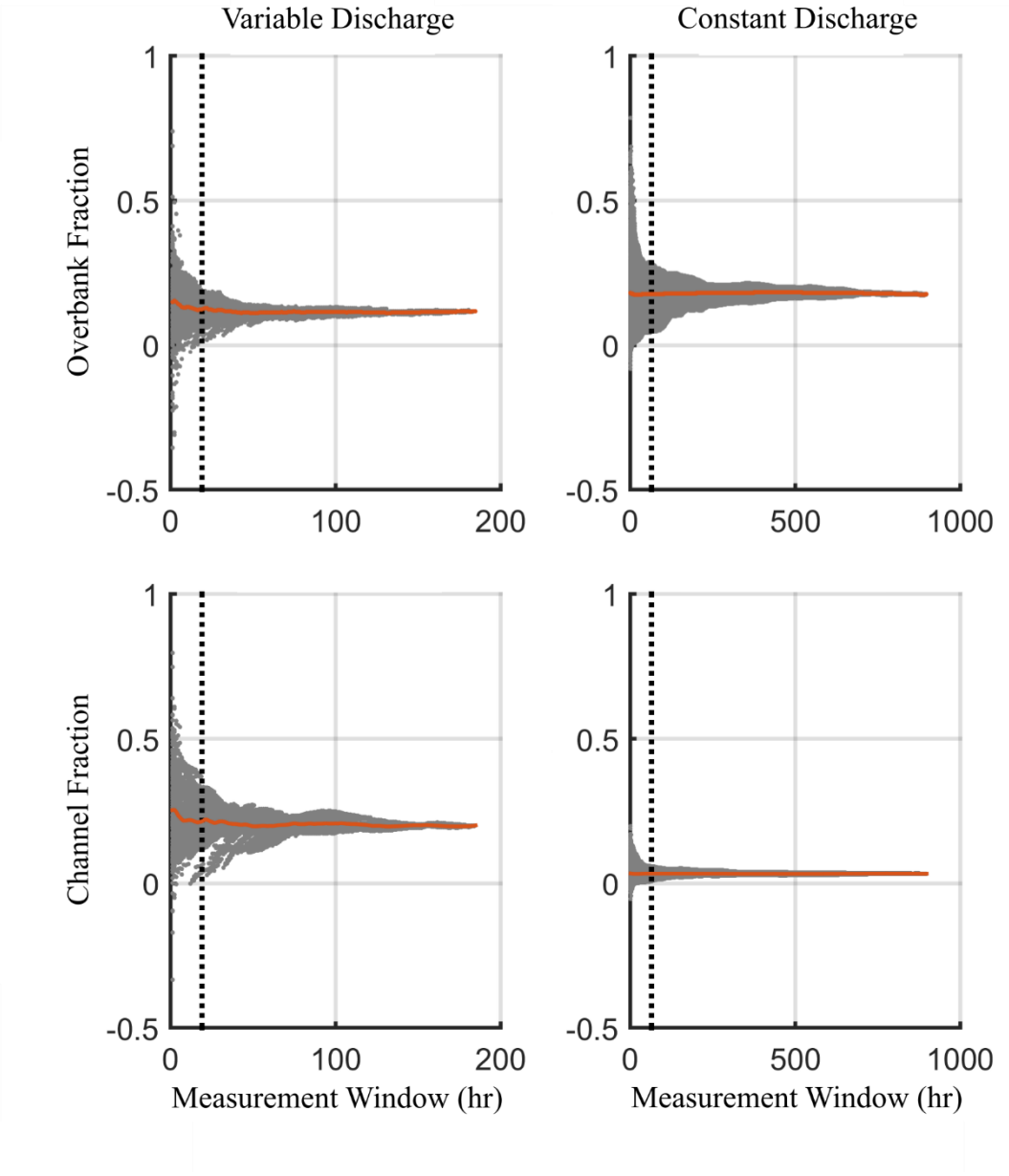

Figure 4-4. Delta Deposit Fraction

The overbank and channel deposit fraction for each delta, displayed as a function of measurement interval. Each grey dot represents the fraction of the total sediment input to the basin during a time period that is preserved as the given deposit type. The average for each measurement window is shown as an orange line. Values below zero indicate net erosion for that environment. The T_5 statistic (Figure 4-6) is shown as a dotted black line. Because these data are calculated as a fraction of sediment input to the basin rather than sediment deposited in the delta top, the magnitudes are lower than those shown in Table 4-2.

We also compute the time of occupation for channel and overbank environments, shown in Figure 4-5. The overbank environment in each experiment occupies the entire delta area with similar frequency, but the pattern of channel occupation is different. The constant flow case shows a small number of channel locations surrounded by a high proportion of delta top area that was never or very rarely occupied by a channel. In the variable flow delta almost every spot on the delta was occupied for a significant amount of time. This is an indication of high mobility of the variable flow channels, which is discussed further below.

To investigate rates of vertical change, we follow the technique of Sheets et al. (2002) and calculate the effective aggradation rate of channel and overbank environments by dividing the total aggradation attributable to one environment at a given location by the occupation time of that same environment. The result of this calculation, displayed in Table 4-2, shows that channels in the variable flow experiment aggrade only slightly more rapidly than those in the constant flow experiment, but that a location on the variable flow delta top is subject to channel aggradation for an average of 22% of the time, which is more than three times as long as the 7% experienced by a location in the constant case. Locations on both deltas are subject to overbank aggradation for approximately the same fraction of time, but the overbank effective aggradation rate is twice as fast in the constant discharge delta (0.43 mm/hr) as in the variable discharge delta (0.2 mm/hr). Time that is not spent as overbank or as channel is spent as either a dry land or a marine environment. The effective aggradation rates shown in Table 4-2, and discussed thus far, are net rates that implicitly include erosion. In Table 4-3 we decompose the effective aggradation rates into pure aggradation and erosion. In this way we see that erosion affects the overbank environment

in both experiments, but that erosion in the variable discharge overbank environment takes place slightly more often (17% of the time, compared to 13%) and operates at substantially higher rates (0.52 mm/hr, compared to 0.27 mm/hr) than in the constant flow case.

Finally, we quantify channel mobility with the normalized overlap statistic introduced by Wickert et al. (2013) (Figure 4-6). This technique measures the amount of time necessary for the channel network to change such that no information about the initial channel pattern is preserved. The key calculation is to compute the number of pixels that have changed between channel and non-channel environments from an initial timestep to a future timestep. We then compute the number of changed pixels that would be expected if the equivalent channel and non-channel areas were randomly distributed in the map of each timestep. A ratio near 1 of the number of pixels that were changed to the number that were expected to be changed randomly indicates that very little information has been preserved, and achieving such a value in a small number of time steps indicates high channel mobility. This ratio, subtracted from 1, is referred to as the Normalized Overlap statistic. As suggested by Wickert et al. (2013), we perform this calculation beginning at each timestep, and measure the average time necessary to get 95% of the way towards no retained information, which we call T_5 (Table 4-1). The T_5 for the constant flow channel network is 64 hours, and is 19 hours for the variable flow case, indicating that the constant flow channels are less mobile, and it therefore takes much longer for their networks to decorrelate.

Our results connect the partitioning of channel vs. overbank deposits to the morphodynamics of the channels. Channels in the constant flow experiment tend to remain in place for long periods of time (Figure 4-5, serial images in SI), resulting in isolated,

vertically aggrading channels. These isolated channels are evident in the preserved stratigraphy (Figure 4-7), as are the natural levee deposits that flank them and the overbank sediments beyond the levees. In this scenario channels act mostly as conduits for sediments to reach the shoreline; the bulk of the aggradation that occurs on the delta top is derived from flow that escapes the main channels. As in the constant flow experiment, the channels in the variable flow experiment aggrade rapidly compared to the overbank environment. However, the channels also move rapidly across the delta top, allowing their deposits to be spread widely. The lateral migration is evident in the map of occupation time (Figure 4-5), and in the channel forms preserved in stratigraphy (Figure 4-7). As a result of this migration, channels in the variable flow experiment leave sediment behind as they move across the delta, and are therefore substantial depositional contributors to stratigraphic volume. The contrast in channel function (conduit vs. depositional contributor) results in more sediment being retained on the delta top in the variable discharge experiment than in the constant flow experiment. We can use our aggradation maps to calculate that the constant flow experiment retains $2.4\times10^{5}\,\frac{mm^{3}}{hr}$ in terrestrial deposits, which is approximately half of the $4.7\times10^{5}\,\frac{mm^{3}}{hr}$ measured in the variable flow experiment. The fact that the variable flow case has a higher sediment retention efficiency and a higher proportion of channel deposits implies that its channel bodies are composed of a lower sand fraction than the constant flow case.

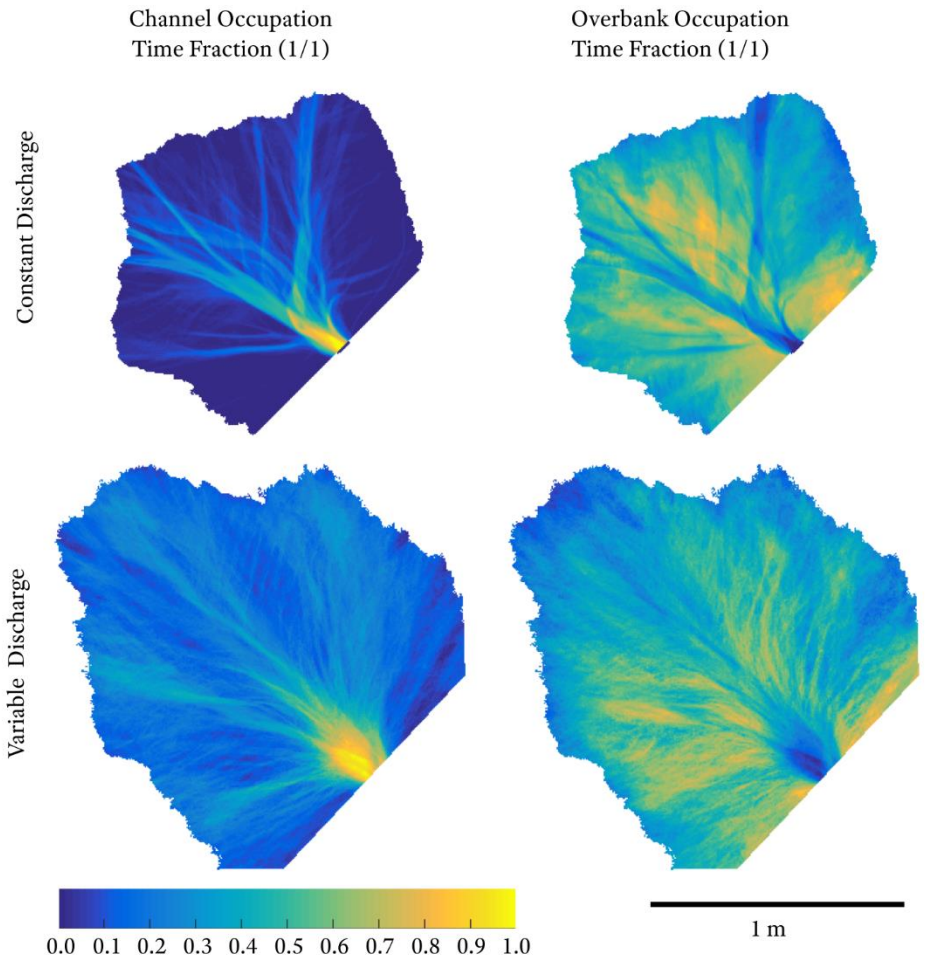

Figure 4-5. Occupation Time

Maps showing the fraction of total run time spent as a channel or as overbank. The variable discharge maps show the entire run time of 186 hours. We used a 186 hour long portion of the constant discharge experiment (hours 500 to 686) for consistency.

		Channels	Overbank
Variable Discharge	aggradation rate (mm/hr)	1.32	0.74
	aggradation time fraction (-)	0.16	0.26
	erosion rate (mm/hr)	0.61	0.52
	erosion time fraction (-)	0.06	0.17
Constant Discharge	aggradation rate (mm/hr)	1.03	0.78
	aggradation time fraction (-)	0.05	0.29
	erosion rate (mm/hr)	0.42	0.27
	erosion time fraction (-)	0.02	0.13

Table 4-3. Aggradation Breakdown

Table showing the effective aggradation rate decomposed into the amount of time spent aggrading or eroding, and the respective rates.

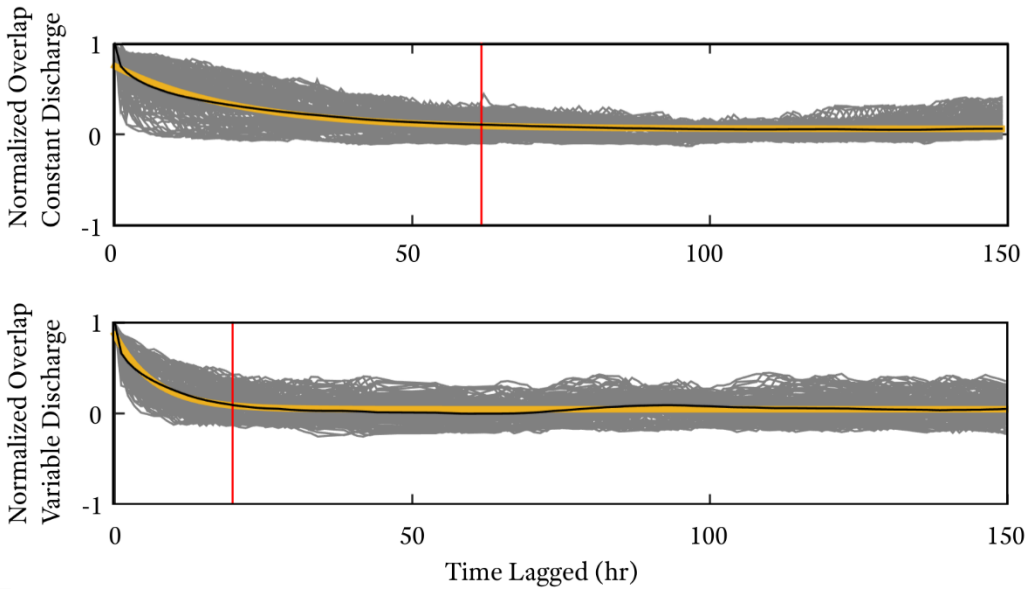

Figure 4-6. Channel Mobility

Normalized overlap decay curves, following Wickert et al (2013). Grey lines are the decay curves described in the text, The black line is the average of the grey lines, and the orange line is the best fit exponential decay to the black line. The vertical red lines, calculated from the orange best fit curves, indicate the T_5 measurement that is shown in Figure 4-4.

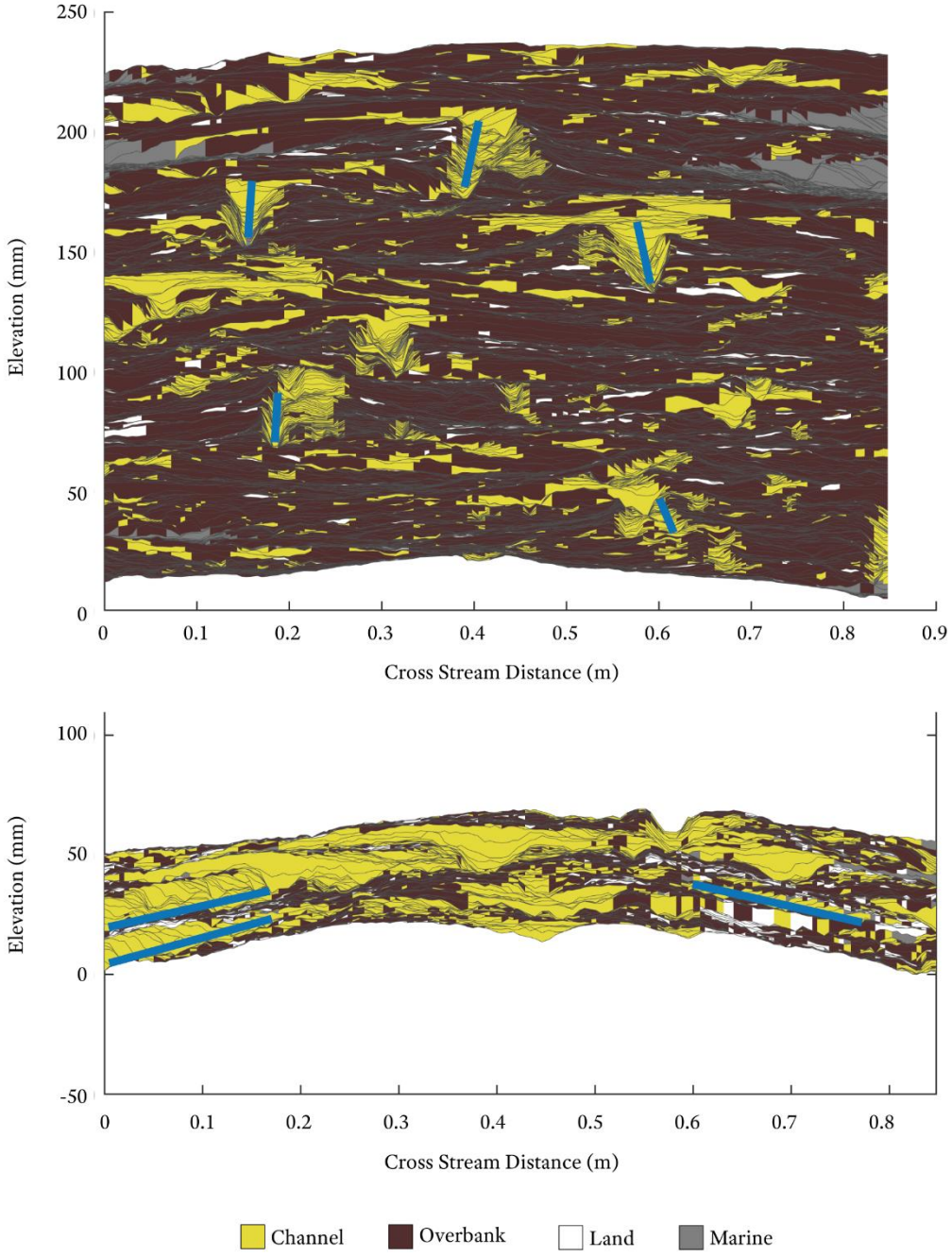

Figure 4-7. Cross Sections

Synthetic stratigraphic cross sections colored by depositional environment. Note the channel thalweg trajectories indicated with blue bars. Cross section locations are shown on Figure 4-2

4.5 Discussion

The principal result of this study is that floods influence channel lateral mobility, which in turn alters the partitioning of sediments between channelized and overbank deposits. This result should hold for alluvial fans, deltas, and any other net depositional environment where regular floods are a driver of channel mobility. That the channels are more mobile in the variable flow experiment can be seen in the statistical evaluation (via T_5, Figure 4-6) as well as by visual examination of the stratigraphy (Figure 4-7) and of the time lapse imagery of the delta (see SI). The increased mobility has a counterintuitive consequence: the deposit of the delta created with floods has a lower proportion of overbank deposits than the one created under constant flow conditions. Though our results are only one data point in a large parameter space, this is a result with broad implications. As noted by Jerolmack and Paola (2007), surprisingly little is known about the rules that govern floodplain sedimentation. Our investigation identifies the intensity of a river's hydrograph as an important parameter that influences sediment export from the channel to the overbank environment. Users of models that derive from the Leeder-Allen-Bridge family can incorporate this information to better ground their model inputs to fluvial processes. For example, the data in Figure 4-4 shows that any measurement of channel to overbank deposit ratio from a time interval that is longer than T_5 should be very close to the long term mean. In our experiments the partitioning of channel and overbank deposition was highly variable over time scales less than T_5. The mean partitioning over these short time scales, however, was close to the long term mean, which suggests that the movement of channels in our experiment was not associated with significant erosion of overbank strata. This might be due to the enhanced deposit cohesion achieved with our sediment mixture. In many systems, erosion of overbank strata, which occurs as a result of channel

lateral migration (van de Lageweg et al., 2014) or incisional avulsions (Hajek and Edmonds, 2014), is common. Significant removal of overbank strata and replacement with channel sediments, from the processes mentioned above, would only further tilt the long time-scale partitioning of sediment towards channelized strata.

As shown in the Results section, differences in channel mobility lead to the differences in sediment partitioning that we observe between our two experiments. The changing flow conditions in our variable discharge experiment ensure that the channel geometry is never in equilibrium with its input. The result is an aggrading channel bed that forces the channel to regularly overflow and invade the adjacent areas. This mechanism, which depends on variable flow and sediment that resists erosion, allows for a rapidly moving channel that does substantial aggradation on the delta top, but little erosion (though still more than in the constant flow overbank environment), and results in a deposit that is dominated by broad, laterally continuous channel bodies (serial images in SI, Figure 4-7). By contrast, the channels in the constant flow experiment lose flow, resulting in the formation of well-developed levees, but the channels are relatively stable and more efficiently pass their sediment from the input all the way to the ocean. The lack of well-developed levees in the variable flow experiment led to channels that were shallower (Table 4-1) and wider (Figure 4-2) than their counterparts formed under constant flow conditions. The contrast between our two experiments is therefore enabled by the cohesive sediment that we use, which allows levees and strong banks to form if energetic flows do not overwhelm them.

Our results, from experiments with cohesive sediment and strong banks, are interesting in the context of two recent studies that examined the impact of flooding on

channel form in braided streams with relatively weak banks. Sambrook (Sambrook Smith et al., 2010) present DEM's collected before and after a large flood (40 year return period, ~10x typical flow conditions) in the South Saskatchewan River. Their data show that the flood significantly altered the planform morphology, but that the new channels were not deeper, nor were the new bars thicker. Because the floods did not alter the total relief in the system, the induced morphological changes would not be easily recognizable in the stratigraphy, implying that floods would not be important to include in forward stratigraphic models of a similar system. The reason the flood was not effective enough to be preserved, Sambrook Smith et al. (2010) found, is that all floods above a certain magnitude lose flow to the overbank environment, resulting in a reduction in stream power. This same line of reasoning should hold with more common floods, making it extremely difficult to distinguish flood intensity by preserved hydraulic geometry alone. Van de Lageweg et al. (2013) confirm experimentally that channel depths and bar thicknesses are not statistically different between a braided stream subject to repeated floods and one with a constant discharge.

Unlike Van de Lageweg et al. (2013)'s braided stream deposits, the stratigraphic products of our two experiments are easily differentiated by the mobility of the channel bodies and by the proportion of channel deposits. The contrast between the two results suggests that information about river dynamics is better preserved in single-threaded systems with cohesive banks than in braided streams in non-cohesive material. This knowledge can be used to select field sites that are likely to yield the most informative data. For example, a stratigrapher interested in a regional shift in precipitation patterns might look for a volumetric change in the density of channel bodies in a single-threaded system.

But if only braided streams in non-cohesive material whose deposits are dominated by channels are available, such an investigation might not be worth undertaking.

4.6 Conclusions

1) Intuition might lead to the assumption that the volume of overbank strata in an alluvial basin increases with the intensity of the floods in the catchment. Results from this study challenge this assumption and suggest that floods can increase channel lateral mobility, which increases the proportion of channel relative to overbank deposits preserved in stratigraphy. We also find that the variable discharge delta retained more total sediment on its delta top than the constant discharge delta. We tie this result to the observation that the channels in the constant discharge delta were stable for long periods of time, during which they functioned as efficient conduits of sediment to the ocean.

2) The T5 statistic, which measures the approximate time necessary for channels to occupy the entire delta top, provides a useful timescale to determine the time interval over which a measurement of channel to overbank sediment partition is representative of the long term average. Measurements from intervals that are shorter than T5 are likely to have an elevated proportion of overbank sediments relative to the long term average. These observations represent an advance in our understanding of the rules that govern long term sediment storage in floodplains, and will be useful to users of rules based models of alluvial stratigraphy formation.

3) Our results differ from those found in studies of braided streams with noncohesive sediment in which no information about hydrograph shape was transferred to the stratigraphy. In contrast to braided systems, where the vast majority of the preserved deposits result from channelized processes, we find that single threaded streams in cohesive

sediment preserve recognizable flood signals in their ratio of preserved overbank to channel deposits.

4.7 APPENDIX

Data from the constant and variable discharge experiments (TDB_12_1, and TDB_15_2, respectively) has been uploaded to the Sustainable Environment – Actionable Data (SEAD) project data repository in collaboration with the Sediment Experimentalist Network. All data can be accessed through the Tulane Sediment Dynamics and Quantitative Stratigraphy Group's collection, at the URL below.

https://sead2.ncsa.illinois.edu/collection/596d28c5e4b05e3417b2096f

5 Conclusions

Each of the three manuscripts that make up this dissertation was intended to answer a fundamental question about how river channels interact with the overbank environments that surround them. Each project was conceived of and executed separately. Each uses different data, and different analysis tools, and each will be published in the academic literature separately. But my hope is that compiled in a single document as they are here, the connections between the works are clear, and their totality is greater than the sum of the parts.

In Chapter 2 my coauthors and I compared the proportion of sand that was preserved in a crevasse splay deposit in the Mississippi River Delta to the hypothesized sand proportion that was carried by the river that fed it during its period of activity. We made the assumption, which is supported by our core data, that all of the sand sized sediments that were exported from the river into the crevasse splay were deposited, and remain, close to the crevasse itself. Thus any loss of retention efficiency must have come from loss of fines to the downstream boundary of the splay. This simple method is surprisingly powerful, and allowed us to answer a question that is critical to coastal restoration and planning efforts in the Mississippi River Delta: what range of sediment retention efficiency can be expected for a land building sediment diversion? The answer to this deceptively simple question seems to be somewhere in the range of 75 to 100%. More

importantly than the specific retention efficiency that we measured at our site, we showed the extreme variability of SRE throughout a delta, and demonstrated the first order importance of depositional setting to sediment retention efficiency. Through a comprehensive catalog of retention efficiencies on a delta is beyond the scope of this work, we showed that deltaic features that are protected from coastal processes are likely to have sediment retention efficiencies as much as an order of magnitude higher than those that are not.

Of course, given the variability in retention efficiency that we identified, the results from any one location are only relevant to small scale features on a delta. In Chapter 4 we took a spatially and temporally broader view by quantifying the sediment storage in the overbank environment across the entire delta top in physical experiments. Here we identified regular flooding as a process that increases channel lateral mobility, and spreads channel deposits more broadly throughout the basin. In an experiment run without floods, the channels developed levees that confined flow and stabilized channel locations. It is important that our experiments were conducted with a cohesive sediment mixture, as the contrast between the stratigraphic products of systems with and without floods does not seem to be significant in systems that are dominated by noncohesive sediments, such as those described by Sambrook Smith et al. (2010) and van de Lagaweg et al. (2013). Our results therefore show that depositional systems dominated by cohesive sediments are more likely to preserve information about past changes in a river's hydrograph within the deposit's geometry. This information will guide site selection for researchers who are interested in studying long term changes to regional precipitation patterns or other climate shifts. It also provides numerical modelers who develop rules based models of basin filling

with information about how they can adapt the rules of their models to better account for surface processes.

While Chapters 2 and 4 both center on sediment preservation in the overbank environment, Chapter 3 is primarily concerned with the effect of the channel/overbank interaction insofar as how flow loss influences the hydrodynamic and sediment transport behavior of the channel. The primary field data set in this chapter is a unique record of synoptic scale hydrodynamic data collected during flood conditions in three terminal distributary networks in the Mississippi River's birdsfoot delta. Using this data for calibration and validation, we adapted a hydrodynamic model of gradually varied flow to account for losses from the channel to the overbank. Doing so allowed us to develop a metric for distributary channel stability, and to demonstrate that flow loss in unmanaged channels is often tuned to maintain a network in a stable configuration. The hydraulic principles of gradually varied flow that govern the response to flow loss in unmanaged terminal distributary channels are the same as those that operate at larger scales in the trunk channels of major rivers in their backwater reach. The lessons that we learned from our data in the terminal distributaries therefore present an opportunity to examine the influence that manmade flood protection levees have had on the channel bed morphology of large, heavily managed rivers like the Mississippi. Applying our model to a hypothetical trunk channel with and without flow losses tells us that building levees along a channel probably lowers the bed elevation throughout the backwater reach, and that the effect is most pronounced towards the shoreline. This is a lesson with significant implications for any researcher who seeks to apply observations from a modern managed river to the stratigraphic record.

Through these documents I have examined the conditions that cause overbank features to effectively retain sediments provided from the river; the ways in which flow loss from the channel to the surrounding environment influences bed evolution and channel network stability in lowland rivers and deltas; and the influence that the character of a river's hydrograph exerts on channel mobility and on the eventual resting place for river-borne sediments. We now know that crevasse splays in protected environments are superbly effective sediment traps if they are protected from coastal processes that could act to strip fine sediments from their deposit. We also now know that flow loss is important to the stability of delta distributary networks, and that overbank deposition isn't necessarily associated with large floods. Each of these observations fits in a broader context of previous research or intuition, but none had been quantified to the extent that my coauthors and I have been able to do here. My hope is that each manuscript can stand fully on its own as an enduring contribution to our knowledge of sedimentary systems, but that considering them together will allow readers a deeper understanding of the range of potential interactions between channels and the overbank environment. Further, I hope that the tools that I have demonstrated here, from a framework to compare transport in rivers to their deposits, to a metric for bifurcation stability, to a process-based method of informing rules-based models, will be of use to future generations of researchers.

6 References

Aalto, R., Maurice-Bourgoin, L., Dunne, T., Montgomery, D. R., Nittrouer, C. A. and Guyot, J.-L.: Episodic sediment accumulation on Amazonian flood plains influenced by El Niño/Southern Oscillation, Nature, 425(6957), 493–497, doi:10.1038/nature02002, 2003.

Allison, A., M. A., Biedenharn, D. S. and Little, C. D.: Suspended Sediment Loads and Tributary Inputs In The Mississippi River Below St. Louis, MO, 1990-2013: A Comparison With the Keown et al. (1981) report., U.S. Army Corps of Engineers, Vicksburg, MS., in review.

Allison, M. A. and Meselhe, E. A.: The use of large water and sediment diversions in the lower Mississippi River (Louisiana) for coastal restoration, J. Hydrol., 387(3–4), 346–360, doi:10.1016/j.jhydrol.2010.04.001, 2010.

Allison, M. A., Kuehl, S. A., Martin, T. C. and Hassan, A.: Importance of flood-plain sedimentation for river sediment budgets and terrigenous input to the oceans: Insights from the Brahmaputra-Jamuna River, Geology, 26(2), 175–178, doi:10.1130/0091-7613(1998)026<0175:IOFPSF>2.3.CO;2, 1998.

Allison, M. A., Demas, C. R., Ebersole, B. A., Kleiss, B. A., Little, C. D., Meselhe, E. A., Powell, N. J., Pratt, T. C. and Vosburg, B. M.: A water and sediment budget for the lower Mississippi–Atchafalaya River in flood years 2008–2010: Implications for sediment discharge to the oceans and coastal restoration in Louisiana, J. Hydrol., 432–433, 84–97, doi:10.1016/j.jhydrol.2012.02.020, 2012.

Allison, M. A., Vosburg, B. M., Ramirez, M. T. and Meselhe, E. A.: Mississippi River channel response to the Bonnet Carré Spillway opening in the 2011 flood and its implications for the design and operation of river diversions, J. Hydrol., 477, 104–118, doi:10.1016/j.jhydrol.2012.11.011, 2013.

Arcement, G. J. and Schneider, V. R.: Guide for selecting Manning's roughness coefficients for natural channels and flood plains, US Government Printing Office Washington, DC. [online] Available from: http://ponce.sdsu.edu/usgs_report_2339.pdf (Accessed 17 February 2017), 1989.

Atlas: The Louisiana State GIS: Digital Elevation Model, Louisiana, [online] Available from: http://atlas.lsu.edu, 2003.

Auerbach, L. W., Goodbred Jr, S. L., Mondal, D. R., Wilson, C. A., Ahmed, K. R., Roy, K., Steckler, M. S., Small, C., Gilligan, J. M. and Ackerly, B. A.: Flood risk of natural and embanked landscapes on the Ganges-Brahmaputra tidal delta plain, Nat. Clim. Change, 5(2), 153–157, doi:10.1038/nclimate2472, 2015.

Barry, J. M.: Rising Tide: The Great Mississippi Flood of 1927 and How it Changed America, 1st Touchstone Ed edition., Simon & Schuster, New York., 1998.

Biedenharn, D. S., Thorne, C. R. and Watson, C. C.: Recent morphological evolution of the Lower Mississippi River, Geomorphology, 34(3), 227–249, 2000.

Blum, M. D. and Roberts, H. H.: Drowning of the Mississippi Delta due to insufficient sediment supply and global sea-level rise, Nat. Geosci., 2(7), 488–491, doi:10.1038/ngeo553, 2009.

Blum, M. D. and Roberts, H. H.: Is sand in the Mississippi River delta a sustainable resource?, Nat. Geosci., 7(12), 851–852, doi:10.1038/ngeo2310, 2014.

Bolla Pittaluga, M., Coco, G. and Kleinhans, M. G.: A unified framework for stability of channel bifurcations in gravel and sand fluvial systems, Geophys. Res. Lett., 42(18), 7521–7536, doi:10.1002/2015GL065175, 2015.

Boyer, M. E., Harris, J. O. and Turner, R. E.: Constructed Crevasses and Land Gain in the Mississippi River Delta, Restor. Ecol., 5(1), 85–92, doi:10.1046/j.1526-100X.1997.09709.x, 1997.

Bridge, J. S. and Leeder, M. R.: A simulation model of alluvial stratigraphy, Sedimentology, 26(5), 617–644, doi:10.1111/j.1365-3091.1979.tb00935.x, 1979.

Caldwell, R. L. and Edmonds, D. A.: The effects of sediment properties on deltaic processes and morphologies: A numerical modeling study, J. Geophys. Res. Earth Surf., 119(5), 2013JF002965, doi:10.1002/2013JF002965, 2014.

Chatanantavet, P., Lamb, M. P. and Nittrouer, J. A.: Backwater controls of avulsion location on deltas, Geophys. Res. Lett., 39(1), doi:10.1029/2011GL050197, 2012.

Coastal Protection and Restoration Authority of Louisiana: Louisiana's Comprehensive Master Plan for a Sustainable Coast, Coastal Protection and Restoration Authority of Louisiana, Baton Rouge, LA., 2017.

Cui, Y. and Parker, G.: Numerical model of sediment pulses and sediment-supply disturbances in mountain rivers, J. Hydraul. Eng. [online] Available from: http://ascelibrary.org/doi/10.1061/(ASCE)0733-9429(2005)131%3A8(646) (Accessed 28 January 2016), 2005.

Davis, D. W.: Crevasses on the lower course of the Mississippi River, in Coastal Zone'93, pp. 360–378, American Society of Civil Engineers, New York, NY, New Orleans, LA., 1993.

Day, G., Dietrich, W. E., Rowland, J. C. and Marshall, A.: The depositional web on the floodplain of the Fly River, Papua New Guinea, J. Geophys. Res. Earth Surf., 113(F1), F01S02, doi:10.1029/2006JF000622, 2008.

Day, J., Cable, J., Lane, R. and Kemp, G.: Sediment Deposition at the Caernarvon Crevasse during the Great Mississippi Flood of 1927: Implications for Coastal Restoration, Water, 8(38), w8020038, doi:10.3390/w8020038, 2016.

Day, J. W., Boesch, D. F., Clairain, E. J., Kemp, G. P., Laska, S. B., Mitsch, W. J., Orth, K., Mashriqui, H., Reed, D. J., Shabman, L., Simenstad, C. A., Streever, B. J., Twilley, R. R., Watson, C. C., Wells, J. T. and Whigham, D. F.: Restoration of the Mississippi Delta:

Lessons from Hurricanes Katrina and Rita, Science, 315(5819), 1679–1684, doi:10.1126/science.1137030, 2007.

Dietrich, W. E.: Settling velocity of natural particles, Water Resour. Res., 18(6), 1615–1626, doi:10.1029/WR018i006p01615, 1982.

E. J Dent: Notes on the mouths of the Mississippi River, USEngineer Office, New Orleans, La., 1921.

Engelund, F. and Hansen, E.: A monograph on sediment transport in alluvial streams, TEKNISKFORLAG Skelbrekgade 4 Copenhagen V, Denmark. [online] Available from: http://repository.tudelft.nl/assets/uuid:81101b08-04b5-4082-9121-861949c336c9/Engelund_Hansen1967.pdf (Accessed 28 January 2016), 1967.

Ericson, J. P., Vörösmarty, C. J., Dingman, S. L., Ward, L. G. and Meybeck, M.: Effective sea-level rise and deltas: Causes of change and human dimension implications, Glob. Planet. Change, 50(1–2), 63–82, doi:10.1016/j.gloplacha.2005.07.004, 2006.

Farrell, K. M.: Sedimentology and facies architecture of overbank deposits of the Mississippi River, False River region, Louisiana, in Recent Developments In Fluvial Sedimentology, pp. 111–120, The Society of Economic Paleontologists and Minerologists., 1987.

Fisk, H. N.: Geological Investigation of The Atchafalaya Basin and The Problem of Mississippi River Diversion, Corps of Engineers, U.S. Army., 1952.

Foreman, B. Z., Heller, P. L. and Clementz, M. T.: Fluvial response to abrupt global warming at the Palaeocene/Eocene boundary, Nature, 491(7422), 92–95, doi:10.1038/nature11513, 2012.

Ganti, V., Chu, Z., Lamb, M. P., Nittrouer, J. A. and Parker, G.: Testing morphodynamic controls on the location and frequency of river avulsions on fans versus deltas: Huanghe (Yellow River), China, Geophys. Res. Lett., 41(22), 2014GL061918, doi:10.1002/2014GL061918, 2014.

Giosan, L., Constantinescu, S., Filip, F. and Deng, B.: Maintenance of large deltas through channelization: Nature vs. humans in the Danube delta, Anthropocene, 1, 35–45, doi:10.1016/j.ancene.2013.09.001, 2013.

Giosan, L., Syvitski, J., Constantinescu, S. and Day, J.: Protect the world's deltas, Nature, 516(7529), 31–33, doi:10.1038/516031a, 2014.

Goodbred, S. L. and Kuehl, S. A.: Floodplain processes in the Bengal Basin and the storage of Ganges–Brahmaputra river sediment: an accretion study using 137Cs and 210Pb geochronology, Sediment. Geol., 121(3–4), 239–258, doi:10.1016/S0037-0738(98)00082-7, 1998.

Hajek, E. A. and Edmonds, D. A.: Is river avulsion style controlled by floodplain morphodynamics?, Geology, 42(3), 199–202, doi:10.1130/G35045.1, 2014.

Hardy, R. J., Lane, S. N. and Yu, D.: Flow structures at an idealized bifurcation: a numerical experiment, Earth Surf. Process. Landf., 36(15), 2083–2096, doi:10.1002/esp.2235, 2011.

Hiatt, M. and Passalacqua, P.: Hydrological connectivity in river deltas: The first-order importance of channel-island exchange: Connectivity in river deltas, Water Resour. Res., 51(4), 2264–2282, doi:10.1002/2014WR016149, 2015.

Hoyal, D. C. J. D. and Sheets, B. A.: Morphodynamic evolution of experimental cohesive deltas, J. Geophys. Res., 114(F2), doi:10.1029/2007JF000882, 2009.

Humphreys, C. A. and Abbot, L. H.: Report upon the physics and hydraulics of the Mississippi River, Corps of Topographical Engineers, United States Army, Washington. [online] Available from: https://books.google.com/books?hl=en&lr=&id=8pBHmrVGIrsC&oi=fnd&pg=PA1&dq=physics+and+hydraulics+of+the+mississippi+river+humphreys+and+abbot&ots=ejW8gwBCgH&sig=g6RpD31_IvgvPnli4TmOXr-I7xs (Accessed 28 April 2017), 1867.

Jankowski, K. L., Törnqvist, T. E. and Fernandes, A. M.: Vulnerability of Louisiana's coastal wetlands to present-day rates of relative sea-level rise., Nat. Commun., 2017.

Jerolmack, D. J. and Mohrig, D.: Conditions for branching in depositional rivers, Geology, 35(5), 463, doi:10.1130/G23308A.1, 2007.

Jerolmack, D. J. and Paola, C.: Complexity in a cellular model of river avulsion, Geomorphology, 91(3–4), 259–270, doi:10.1016/j.geomorph.2007.04.022, 2007.

Jerolmack, D. J. and Swenson, J. B.: Scaling relationships and evolution of distributary networks on wave-influenced deltas, Geophys. Res. Lett., 34(23), L23402, doi:10.1029/2007GL031823, 2007.

Kemp, G. P., Day, J. W., Rogers, J. D., Giosan, L. and Peyronnin, N.: Enhancing mud supply from the Lower Missouri River to the Mississippi River Delta USA: Dam bypassing and coastal restoration, Estuar. Coast. Shelf Sci., doi:10.1016/j.ecss.2016.07.008, 2016.

Keown, M. P., Dardeau, E. A. and Causey, E. M.: Historic Trends in the Sediment Flow Regime of the Mississippi River, Water Resour. Res., 22(11), 1555–1564, doi:10.1029/WR022i011p01555, 1986.

Kesel, R.: The Decline in the Suspended-Load of the Lower Mississippi River and Its Influence on Adjacent Wetlands, Environ. Geol. Water Sci., 11(3), 271–281, doi:10.1007/BF02574816, 1988.

Kim, W., Mohrig, D., Twilley, R., Paoa, C. and Parker, G.: Land Building in the Delta of the Mississippi River: Is it Feasible?, in Coastal Louisiana Ecosystem Assessment & Restoration (CLEAR) Program: A tool to support coastal restoration., vol. IV, Department of Natural Resources, Coastal Restoration Division, Baton Rouge, LA., 2008.

Kim, W., Mohrig, D., Twilley, R., Paola, C. and Parker, G.: Is it feasible to build new land in the Mississippi River Delta?, EOS Trans. Am. Geophys. Union, 90(42), 373–374, 2009.

Kleinhans, M. G., Cohen, K. M., Hoekstra, J. and IJmker, J. M.: Evolution of a bifurcation in a meandering river with adjustable channel widths, Rhine delta apex, The Netherlands, Earth Surf. Process. Landf., 36(15), 2011–2027, doi:10.1002/esp.2222, 2011.

Kleinhans, M. G., Ferguson, R. I., Lane, S. N. and Hardy, R. J.: Splitting rivers at their seams: bifurcations and avulsion, Earth Surf. Process. Landf., 38(1), 47–61, doi:10.1002/esp.3268, 2013.

van de Lageweg, W. I., van Dijk, W. M., Baar, A. W., Rutten, J. and Kleinhans, M. G.: Bank pull or bar push: What drives scroll-bar formation in meandering rivers?, Geology, 42(4), 319–322, doi:10.1130/G35192.1, 2014.

Lamb, M. P., Nittrouer, J. A., Mohrig, D. and Shaw, J.: Backwater and river plume controls on scour upstream of river mouths: Implications for fluvio-deltaic morphodynamics, J. Geophys. Res., 117(F1), doi:10.1029/2011JF002079, 2012.

Leeder, M. R.: A quantitative stratigraphic model for alluvium, with special reference to channel deposit density and interconnectedness, in Fluvial Sedimentology: Memoir, pp. 587–596, Canadian Society of Petroleum Geologists., 1978.

Lewin, J., Ashworth, P. J. and Strick, R. J. P.: Spillage sedimentation on large river floodplains: Spillage sedimentation on large river floodplains, Earth Surf. Process. Landf., doi:10.1002/esp.3996, 2016.

Li, Q., Yu, L. and Straub, K. M.: Storage thresholds for relative sea-level signals in the stratigraphic record, Geology, 44(3), 179–182, doi:10.1130/G37484.1, 2016.

Mackey, S. D. and Bridge, J. S.: Three-Dimensional Model of Alluvial Stratigraphy: Theory and Application, J. Sediment. Res., 65(1) [online] Available from: http://archives.datapages.com/data/sepm/journals/v63-66/data/065b/065b001/0007.htm (Accessed 4 February 2017), 1995.

Meselhe, E. A., Georgiou, I., Allison, M. A. and McCorquodale, J. A.: Numerical modeling of hydrodynamics and sediment transport in lower Mississippi at a proposed delta building diversion, J. Hydrol., 472, 340–354, doi:10.1016/j.jhydrol.2012.09.043, 2012.

Meselhe, E. A., Sadid, K. M. and Allison, M. A.: Riverside morphological response to pulsed sediment diversions, Geomorphology, 270, 184–202, doi:10.1016/j.geomorph.2016.07.023, 2016.

Miori, S., Hardy, R. J. and Lane, S. N.: Topographic forcing of flow partition and flow structures at river bifurcations, Earth Surf. Process. Landf., 37(6), 666–679, doi:10.1002/esp.3204, 2012.

Mississippi River Commission: Preliminary Map of The Lower Mississippi River From The Mouth of The Ohio River to The Head of The Passes. Sheet No. 32, 1885.

Mohrig, D., Heller, P. L., Paola, C. and Lyons, W. J.: Interpreting avulsion process from ancient alluvial sequences: Guadalope-Matarranya system (northern Spain) and Wasatch Formation (western Colorado), Geol. Soc. Am. Bull., 112(12), 1787–1803, doi:10.1130/0016-7606(2000)112<1787:IAPFAA>2.0.CO;2, 2000.

Mueller, D. S., Wagner, C. R., Rehmel, M. S., Oberg, K. A. and Rainville, F.: Measuring discharge with acoustic Doppler current profilers from a moving boat, US Department of the

Interior, US Geological Survey. [online] Available from: http://pubs.usgs.gov/tm/3a22/ (Accessed 15 August 2016), 2009.

Nardin, W. and Edmonds, D. A.: Optimum vegetation height and density for inorganic sedimentation in deltaic marshes, Nat. Geosci., 7(10), 722–726, doi:10.1038/ngeo2233, 2014.

Nicholas, A. P., Sambrook Smith, G. H., Amsler, M. L., Ashworth, P. J., Best, J. L., Hardy, R. J., Lane, S. N., Orfeo, O., Parsons, D. R., Reesink, A. J. H., Sandbach, S. D., Simpson, C. J. and Szupiany, R. N.: The role of discharge variability in determining alluvial stratigraphy, Geology, 44(1), 3–6, doi:10.1130/G37215.1, 2016.

Nittrouer, C. A., Kuehl, S. A., Sternberg, R. W., Figueiredo Jr., A. G. and Faria, L. E. C.: An introduction to the geological significance of sediment transport and accumulation on the Amazon continental shelf, Mar. Geol., 125(3–4), 177–192, doi:10.1016/0025-3227(95)00075-A, 1995.

Nittrouer, J. A. and Viparelli, E.: Reply to "Is sand in the Mississippi River delta a sustainable resource?," Nat. Geosci., 7(12), 852–852, doi:10.1038/ngeo2311, 2014a.

Nittrouer, J. A. and Viparelli, E.: Sand as a stable and sustainable resource for nourishing the Mississippi River delta, Nat. Geosci., 7(5), 350–354, doi:10.1038/ngeo2142, 2014b.

Nittrouer, J. A., Allison, M. A. and Campanella, R.: Bedform transport rates for the lowermost Mississippi River, J. Geophys. Res., 113(F03004), doi:10.1029/2007JF000795, 2008.

Nittrouer, J. A., Mohrig, D. and Allison, M.: Punctuated sand transport in the lowermost Mississippi River, J. Geophys. Res. Earth Surf., 116(F04025), doi:10.1029/2011JF002026, 2011.

Nittrouer, J. A., Best, J. L., Brantley, C., Cash, R. W., Czapiga, M., Kumar, P. and Parker, G.: Mitigating land loss in coastal Louisiana by controlled diversion of Mississippi River sand, Nat. Geosci., 5(8), 534–537, doi:10.1038/ngeo1525, 2012a.

Nittrouer, J. A., Shaw, J., Lamb, M. P. and Mohrig, D.: Spatial and temporal trends for water-flow velocity and bed-material sediment transport in the lower Mississippi River, Geol. Soc. Am. Bull., 124(3–4), 400–414, doi:10.1130/B30497.1, 2012b.

NOAA: Chandeleur and Breton Sounds. Coastal Chart 11363, 2011a.

NOAA: Mississippi River Delta. Coastal Chart 11361, 2011b.

Paola, C., Twilley, R. R., Edmonds, D. A., Kim, W., Mohrig, D., Parker, G., Viparelli, E. and Voller, V. R.: Natural Processes in Delta Restoration: Application to the Mississippi Delta, Annu. Rev. Mar. Sci., 3(1), 67–91, doi:10.1146/annurev-marine-120709-142856, 2011.

Pebesma, E. J.: Multivariable geostatistics in S: the gstat package, Comput. Geosci., 30(7), 683–691, 2004.

Plink-Björklund, P.: Morphodynamics of rivers strongly affected by monsoon precipitation: Review of depositional style and forcing factors, Sediment. Geol., 323, 110–147, doi:10.1016/j.sedgeo.2015.04.004, 2015.

Ramirez, M. T. and Allison, M. A.: Suspension of bed material over sand bars in the Lower Mississippi River and its implications for Mississippi delta environmental restoration, J. Geophys. Res. Earth Surf., 118(2), 1085–1104, doi:10.1002/jgrf.20075, 2013.

Ramirez, M. T., Smith, S. J., Lewis, J. W. and Pratt, T. C.: Mississippi River Bedform Roughness and Streamflow Conditions near Vicksburg, MS, U.S. Army Corps of Engineers Research and Development Center, Vicksburg, MS., (in review).

Rijke, J., Herk, S. van, Zevenbergen, C. and Ashley, R.: Room for the River: delivering integrated river basin management in the Netherlands, Int. J. River Basin Manag., 10(4), 369–382, doi:10.1080/15715124.2012.739173, 2012.

Rittenour, T. M., Blum, M. D. and Goble, R. J.: Fluvial evolution of the lower Mississippi River valley during the last 100 k.y. glacial cycle: Response to glaciation and sea-level change, Geol. Soc. Am. Bull., 119(5–6), 586–608, doi:10.1130/B25934.1, 2007.

Roberts, H. H.: Evolution of Sedimentary Architecture and Surface Morphology: Atchafalaya and Wax Lake Deltas, Louisiana (1973-1994), Gulf Coast Assoc Geol Soc Trans., 47, 477–484, 1997.

Roberts, H. H., Coleman, J. M., Bentley, S. J. and Walker, N.: An embryonic major delta lobe: A new generation of delta studies in the Atchafalaya-Wax Lake delta system, Gulf Coast Assoc Geol Soc Trans., 53, 690–703, 2003.

Roberts, H. H., DeLaune, R. D., White, J., Li, C., Braud, D. and Weeks, E.: Delta Development and Coastal Marsh Accretion During Cold Front Passages and River Floods: Relevance to River Diversions – Final Report, Coastal Studies Institute, Louisiana State University, Baton Rouge, LA., 2016.

Rouse, H.: Modern Conceptions of the Mechanics of Fluid Turbulence, American Society of Civil Engineers., 1936.

Rowland, J. C. and Dietrich, W. E.: The evolution of a tie channel, River Coast. Estuar. Morphodynamics RCEM, 1, 725–736, 2005.

Sambrook Smith, G. H., Best, J. L., Ashworth, P. J., Lane, S. N., Parker, N. O., Lunt, I. A., Thomas, R. E. and Simpson, C. J.: Can we distinguish flood frequency and magnitude in the sedimentological record of rivers?, Geology, 38(7), 579–582, doi:10.1130/G30861.1, 2010.

Scholes, J. R., Betts, R., Bunn, S., Leadley, P., Nepstad, D., Overpeck, J. T. and Taboada, M. A.: Terrestrial and inland water systems, in Climate Change 2014: Impacts, Adaptation, and Vulnerability. Part A: Global and Sectoral Aspects. Contribution of Working Group II to the Fifth Assessment Report of the Intergovernmental Panel on Climate Change, edited by C. B. Fields, V. R. Barros, D. J. Dokken, K. J. Mach, M. D. Mastrandrea, T. E. Bilir, M. Chatterjee, K. L. Ebi, Y. O. Estrada, R. C. Genova, B. Girma, E. S. Kissel, A. N. Levy, S. MacCraken, P. R. Mastrandrea, and L. L. White, Cambridge University Press, Cambridge,

United Kingdom. [online] Available from: https://www.ipcc.ch/pdf/assessment-report/ar5/wg2/WGIIAR5-Chap4_FINAL.pdf (Accessed 24 February 2017), 2014.

Sharp, J., Little, C., Brown, G., Pratt, T., Heath, R., Hubbard, L., Pinkard, F., Martin, K., Clifton, N., Perkey, D. and Ganesh, N.: West Bay Sediment Diversion Effects, US Army Corps of Engineers, Coastal and Hydraulics Laboratory, Vicksburg, MS., 2013.

Shaw, J. B. and Mohrig, D.: The importance of erosion in distributary channel network growth, Wax Lake Delta, Louisiana, USA, Geology, 42(1), 31–34, doi:10.1130/G34751.1, 2014.

Shaw, J. B., Mohrig, D. and Wagner, R. W.: Flow patterns and morphology of a prograding river delta, J. Geophys. Res. Earth Surf., 2015JF003570, doi:10.1002/2015JF003570, 2016.

Sheets, B. A., Hickson, T. A. and Paola, C.: Assembling the stratigraphic record: depositional patterns and time-scales in an experimental alluvial basin, Basin Res., 14(3), 287–301, doi:10.1046/j.1365-2117.2002.00185.x, 2002.

Shen, Z., Törnqvist, T. E., Mauz, B., Chamberlain, E. L., Nijhuis, A. G. and Sandoval, L.: Episodic overbank deposition as a dominant mechanism of floodplain and delta-plain aggradation, Geology, 43(10), 875–878, doi:10.1130/G36847.1, 2015.

Slingerland, R. and Smith, N. D.: Necessary conditions for a meandering-river avulsion, Geology, 26(5), 435–438, doi:10.1130/0091-7613(1998)026<0435:NCFAMR>2.3.CO;2, 1998.

Slingerland, R. and Smith, N. D.: River Avulsions and Their Deposits, Annu. Rev. Earth Planet. Sci., 32(1), 257–285, doi:10.1146/annurev.earth.32.101802.120201, 2004.

Smith, J. E., Bentley, S. J., Snedden, G. A. and White, C.: What Role do Hurricanes Play in Sediment Delivery to Subsiding River Deltas?, Sci. Rep., 5, 17582, doi:10.1038/srep17582, 2015.

Smith, N., Cross, T. A., Dufficy, J. P. and Clough, S. R.: Anatomy of an avulsion, Sedimentology, 36(1), 1, 1989.

Straub, K. M., Paola, C., Mohrig, D., Wolinsky, M. A. and George, T.: Compensational Stacking of Channelized Sedimentary Deposits, J. Sediment. Res., 79(9), 673–688, doi:10.2110/jsr.2009.070, 2009.

Straub, K. M., Li, Q. and Benson, W. M.: Influence of sediment cohesion on deltaic shoreline dynamics and bulk sediment retention: A laboratory study, Geophys. Res. Lett., 42(22), 9808–9815, doi:10.1002/2015GL066131, 2015.

Sutfin, N. A., Wohl, E. E. and Dwire, K. A.: Banking carbon: a review of organic carbon storage and physical factors influencing retention in floodplains and riparian ecosystems: BANKING CARBON, Earth Surf. Process. Landf., 41(1), 38–60, doi:10.1002/esp.3857, 2016.

Tal, M. and Paola, C.: Dynamic single-thread channels maintained by the interaction of flow and vegetation, Geology, 35(4), 347–350, doi:10.1130/G23260A.1, 2007.

The Coast And Geodetic Survey: Mississippi River From The Passes To Grand Prarie, 1906.

Törnqvist, T. E. and Bridge, J. S.: Spatial variation of overbank aggradation rate and its influence on avulsion frequency, Sedimentology, 49(5), 891–905, 2002.

Törnqvist, T. E., Kidder, T. R., Autin, W. J., Borg, K. van der, Jong, A. F. M. de, Klerks, C. J. W., Snijders, E. M. A., Storms, J. E. A., Dam, R. L. van and Wiemann, M. C.: A Revised Chronology for Mississippi River Subdeltas, Science, 273(5282), 1693–1696, doi:10.2307/2891996, 1996.

Törnqvist, T. E., Paola, C., Parker, G., Liu, K., Mohrig, D., Holbrook, J. M. and Twilley, R. R.: Comment on "Wetland Sedimentation from Hurricanes Katrina and Rita," Science, 316(5822), 201b, doi:10.1126/science.1136780, 2007.

Törnqvist, T. E., Wallace, D. J., Storms, J. E. A., Wallinga, J., van Dam, R. L., Blaauw, M., Derksen, M. S., Klerks, C. J. W., Meijneken, C. and Snijders, E. M. A.: Mississippi Delta subsidence primarily caused by compaction of Holocene strata, Nat. Geosci., 1(3), 173–176, doi:10.1038/ngeo129, 2008.

Tucker, C. J.: Red and photographic infrared linear combinations for monitoring vegetation, Remote Sens. Environ., 8(2), 127–150, 1979.

Tweel, A. W. and Turner, R. E.: Watershed land use and river engineering drive wetland formation and loss in the Mississippi River birdfoot delta, Limnol. Oceanogr., 57(1), 18–28, doi:10.4319/lo.2012.57.1.0018, 2012.

U.S. Department of Commerce: Mississippi River Delta, Chart 1272, 1965.

Van de Lageweg, W. I., Dijk, W. M. V. and Kleinhans, M. G.: Morphological and Stratigraphical Signature of Floods In A Braided Gravel-Bed River Revealed From Flume Experiments, J. Sediment. Res., 83(11), 1033–1046, doi:10.2110/jsr.2013.70, 2013.

Wang, Y., Straub, K. M. and Hajek, E. A.: Scale-dependent compensational stacking: An estimate of autogenic time scales in channelized sedimentary deposits, Geology, 39(9), 811–814, doi:10.1130/G32068.1, 2011.

Welder, F.: Processes of deltaic sedimentation in the lower Mississippi River, Technical Report, Louisiana State University, Coastal Studies Institute, Baton Rouge, Louisiana., 1959.

Wickert, A. D., Martin, J. M., Tal, M., Kim, W., Sheets, B. and Paola, C.: River channel lateral mobility: metrics, time scales, and controls, J. Geophys. Res. Earth Surf., 118(2), 396–412, doi:10.1029/2012JF002386, 2013.

Wright, S. and Parker, G.: Modeling downstream fining in sand-bed rivers. I: formulation, J. Hydraul. Res., 43(6), 613–620, doi:10.1080/00221680509500381, 2005a.

Wright, S. and Parker, G.: Modeling downstream fining in sand-bed rivers. II: application, J. Hydraul. Res., 43(6), 621–631, doi:10.1080/00221680509500382, 2005b.

Xu, K., Bentley, S. J., Robichaux, P., Sha, X. and Yang, H.: Implications of Texture and Erodibility for Sediment Retention in Receiving Basins of Coastal Louisiana Diversions, Water, 8(26), w8010026, doi:10.3390/w8010026, 2016.

Biography

Christopher Esposito received a B.S. in Mathematics and Physical Oceanography from Rutgers, The State University of New Jersey in 2003, and an M.S. in Earth and Environmental Sciences from the University of New Orleans in 2011. He is currently a Research Scientist at The Water Institute of The Gulf.